

3

Real Reactors and Residence Time Distribution (RTD)

In Chapter 2, the design of the so-called “ideal reactors” was discussed. The reactor “ideality” was based on defined hydrodynamic behavior. We had assumed two flow patterns: plug flow (piston type) where axial dispersion is excluded and completely mixed flow achieved in ideal stirred tank reactors. These flow patterns are often used for reactor design because the mass and heat balances are relatively simple to treat. But real equipment often deviates from that of the ideal flow pattern. In tubular reactors radial velocity and concentration profiles may develop in laminar flow. In turbulent flow, velocity fluctuations can lead to an axial dispersion. In catalytic packed bed reactors, irregular flow with the formation of channels may occur while stagnant fluid zones (dead zones) may develop in other parts of the reactor. Incompletely mixed zones and thus inhomogeneity can also be observed in CSTR, especially in the cases of viscous media.

The abovementioned phenomena lead to a nonuniform residence time of the fluid elements in tubular reactors, which may have a detrimental effect on the reactor performance and product yield.

In this chapter, residence time distribution (RTD) of ideal and nonideal reactors along with the method of determination are described in detail. The influence of nonideality and RTD on the reactor performance, the target product yield, and selectivity, including complex reactions, is presented.

3.1

Nonideal Flow Pattern and Definition of RTD

Herein, only the steady-state flow without any reaction and without density changes ($\dot{V}_0 = \dot{V}_{\text{out}}$) of a single fluid flow through an open vessel is considered.

In order to design a flow reactor rationally, one needs to know how long the individual molecules stay in the vessel (the residence time). If for the ideal plug flow reactor all molecules come in and go out together (piston type flow pattern) meaning that the residence time is the same for the whole reacting mixture, in real reactors some elements of the fluid may have different pathways resulting in

different time to pass through the reactor. The distribution of these times is called the *residence time distribution (RTD)*. The RTD of a fluid can be characterized by the age distribution of volume elements $E(t)$, which have left the reactor. A typical RTD characterized by the function $E(t)$ is shown in Figure 3.1. The function $E(t)$ indicates the probability that a fraction of the total amount (n_0) entering the reactor at $t = 0$ has left the reactor after the time t . The dimension of $E(t)$ is s^{-1} .

$$E(t) = \frac{\dot{n}(t)}{n_0} = \frac{\dot{V}c(t)}{\int_0^\infty \dot{V}c(t)dt} \quad (3.1)$$

After an infinitely long observation time, the probability that all volume elements fed into the reactor at the time $t = 0$ have left is equal to one.

$$\int_0^\infty E(t)dt = 1 \quad (3.2)$$

The fraction of the fluid in the exit stream, which is younger than t_1 , corresponds to

$$\int_0^{t_1} E(t)dt \quad (3.3)$$

and that which is older to

$$\int_{t_1}^\infty E(t)dt = 1 - \int_0^{t_1} E(t)dt \quad (3.4)$$

It is often advantageous to relate the distribution functions to the mean residence time in order to be able to compare reactors of different sizes and with different throughputs. Thus, a dimensionless time referred to the mean residence time is introduced.

$$\theta = t/\bar{t} \quad (3.5)$$

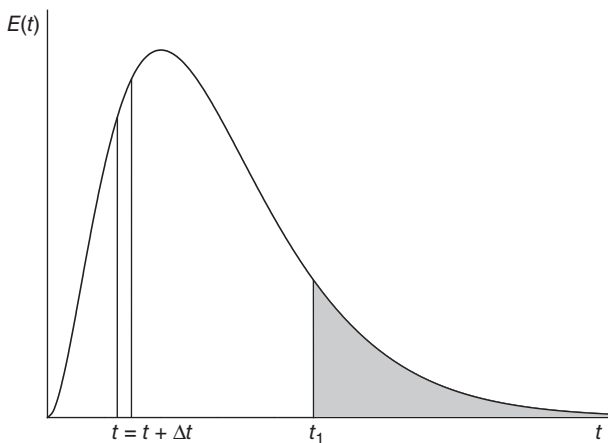


Figure 3.1 Residence time distribution, or exit age distribution curve, $E(t)$.

We then obtain the following relationships for the distribution functions

$$E(\theta) \equiv E = \bar{t} \cdot E(t) \quad (3.6)$$

For practical purposes, it is beneficial to characterize distribution functions by a few characteristic terms as the mean residence time and the variance around the mean. The mean residence time (\bar{t}) corresponds to the first moment of the distribution function, $E(t)$.

$$\mu_1 = \bar{t} = \int_0^{\infty} t \cdot E(t) dt \quad (3.7)$$

If the density of the fluid does not change in the reactor ($\dot{V}_0 = \dot{V}_{\text{out}}$), the mean residence time corresponds to the space time.

$$\bar{t} = \tau = V/\dot{V}_0; \rho = \text{const} \quad (3.8)$$

The variance of the distribution is obtained from the second moment of the distribution function.

$$\sigma^2 = \mu_2 - \mu_1^2 = \int_0^{\infty} t^2 \cdot E(t) dt - \bar{t}^2 = \int_0^{\infty} (t - \bar{t})^2 E(t) dt \quad (3.9)$$

The skewness (sk) is a measure for the deviation from the symmetrical distribution. It is characterized by the third moment of the distribution defined with Equation 3.10 [1].

$$\text{sk} = (\mu_3 - 2\mu_1^3 - 3\mu_1\mu_2)/\sigma^3 = \int_0^{\infty} (t - \bar{t})^3 E(t) dt / \sigma^3 \quad (3.10)$$

The higher moments of the RTD are of little practical interest because they are difficult to obtain experimentally with the required accuracy.

3.2

Experimental Determination of RTD in Flow Reactors

To determine the RTD experimentally, widely used stimulus-response methods are applied. For this an inert tracer is introduced at the inlet of the reactor. The response of the system to the imposed inlet perturbation is obtained by measuring the tracer concentration at the reactor outlet as function of time. It is important that the tracer does not change the physical properties of the fluid, that is, viscosity and density of the fluid must remain constant. In addition, the tracer should not take part in the reaction process, not be adsorbed at parts of the reactor; furthermore, it should be easy to measure even in low concentrations.

Usually, the tracer is injected in the form of a well-defined function: as a step or impulse function, and sometimes in the form of a sinus function. The first two functions are used mostly and are discussed in detail.

3.2.1

Step Function Stimulus-Response Method

At the inlet of the reactor, the concentration of a tracer is abruptly changed at time $t=0$. In practice, the stepwise change should be faster than a hundreds of the space time in the reactor ($\Delta t_{\text{step}} < 0.01\tau$). The response of the system at the reactor outlet is measured. The momentary tracer concentration $c(t)$ is referred to the constant inlet concentration c_0 . The response curve is thus dimensionless and is designated as an F -curve according to Danckwerts [2, 3]; it thus has values between 0 and 1 (see Figure 3.2) and corresponds to the cumulative curve of the RTD.

$$F(t) = \frac{c(t)}{c_0} \quad (3.11)$$

The following relationship between the external RTD and the F -curve holds:

$$F(t) = \int_0^t E(t') dt' = \int_0^\theta E d\theta' = F \quad (3.12)$$

$$E(t) = \frac{dF(t)}{dt} = \frac{dF}{d\theta} \quad (3.13)$$

The mean residence time in the reactor is obtained from the F -curve according to

$$\bar{t} = \int_0^\infty t \cdot E(t) dt = \int_0^1 t \cdot dF \quad (3.14)$$

or with discrete measurement points

$$\bar{t} \approx \sum_i t_i \cdot \Delta F_i \quad (3.15)$$

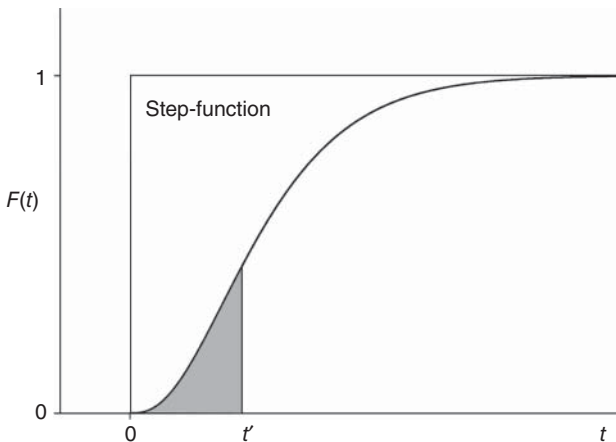


Figure 3.2 Response at the reactor outlet on a tracer introduced as a step function at the reactor inlet.

In analogy, the variance is obtained with

$$\begin{aligned}\sigma^2 &= \int_0^{\infty} (t - \bar{t})^2 E(t) dt = \int_0^{\infty} t^2 E(t) dt - \bar{t}^2 \\ \sigma^2 &= \int_0^1 (t - \bar{t})^2 dF\end{aligned}\quad (3.16)$$

or with discrete measured points

$$\sigma^2 \simeq \sum_i (t_i - \bar{t})^2 \Delta F_i \quad (3.17)$$

In general the tracer concentrations are measured at constant time intervals, Δt . Therefore, it may be preferable to carry out the integration over the time. Transformation of Equation 3.14 leads to [4]:

$$\bar{t} = \int_0^1 t \cdot dF = - \int_0^1 t \cdot d(1 - F) = \int_0^{\infty} (1 - F) dt \quad (3.18)$$

Equation 3.16 can be transformed accordingly.

$$\sigma^2 = \int_0^1 (t - \bar{t})^2 dF = \int_0^1 t^2 dF - \bar{t}^2 = 2 \int_0^{\infty} t \cdot (1 - F) dt - \bar{t}^2 \quad (3.19)$$

3.2.2

Pulse Function Stimulus-Response Method

The entire amount of the tracer is fed to the reactor inlet within a very short time to approach the Dirac delta function as close as possible. The Dirac function has the following properties:

$$\begin{aligned}t = 0 \quad \delta(t) &= \infty \\ t \neq 0 \quad \delta(t) &= 0 \\ \int_{-\infty}^{+\infty} \delta(t) dt &= 1\end{aligned}\quad (3.20)$$

In practice, the input time Δt_{pulse} should be small compared to the space time ($\Delta t_{\text{pulse}} \leq 0.01\tau$). The response at the reactor outlet to the pulse-like tracer injection is called the *C-curve*. The *C-curve* is experimentally determined by measuring the tracer concentration at the outlet following the inlet pulse. The measured values are referred to the total amount of tracer injected.

$$C(t) = \frac{\dot{n}(t)}{n_{inj}} = \frac{\dot{V}_{out} c(t)}{\int_0^{\infty} \dot{V}_{out} c(t) dt} = \frac{c(t)}{\int_0^{\infty} c(t) dt}; \quad \dot{V}_{out} = const. \quad (3.21)$$

The experimental *C-curve* corresponds to the RTD defined in Equation 3.1 for systems closed for dispersion (see Section 3.4.2). In this case $C(t) = E(t)$.

The same holds for the mean residence time:

$$\begin{aligned}\bar{t}_C &= \int_0^{\infty} t \cdot C(t) dt = \bar{t} = \tau; \\ &\text{closed for dispersion, constant density}\end{aligned}\quad (3.22)$$

The same is true for the variance around the mean:

$$\sigma_C^2 = \int_0^{\infty} (t - \bar{t}_C)^2 \cdot C(t) dt = \sigma^2;$$

closed for dispersion, constant density (3.23)

The estimation of mean residence time and variance are illustrated in Example 3.1. The situation is different for systems open for dispersion as discussed in Section 3.4.2. Under these conditions the experimentally determined C -curve is not identical with $E(t)$:

$$\left. \begin{array}{l} C(t) \neq E(t) \\ \bar{t}_c \neq \bar{t} \end{array} \right\} \text{systems open for dispersion} \quad (3.24)$$

Example 3.1: Experimental determination of RTD

The RTD of a tubular reactor is measured with the pulse function stimulus-response method. The experimental results are summarized in Table 3.1:

Table 3.1 Experimental response to a pulse function.

t (s)	0	120	240	360	480	600	720	840	960
$c(t)$ (kg · m ⁻³)	0	6.5	12.5	12.5	10.0	5.0	2.5	1.0	0

Calculate the values of \bar{t}_C and σ_C^2 and plot the $C(t)$ and F -curve versus θ_C .

Solution:

1) $\int_0^{\infty} c(t) dt \cong \sum c_i \Delta t_i = 6000 \text{ kg m}^{-3} \text{ s}$ using the mean concentrations in the various Δt intervals

2) $\int_0^{\infty} t c(t) dt \cong \sum t_i c_i \Delta t_i = 2\,246\,400 \text{ kg m}^{-3} \text{ s}^2$

3) $\int_0^{\infty} t^2 c(t) dt \cong \sum t_i^2 c_i \Delta t_i = 1.025 \cdot 10^9 \text{ kg m}^{-3} \text{ s}^3$.

$$\bar{t}_C = \frac{\sum t_i c_i \Delta t_i}{\sum c_i \Delta t_i} = 374.4 \text{ s}$$

$$\sigma_C^2 = \frac{\sum t_i^2 c_i \Delta t_i}{\sum c_i \Delta t_i} - \bar{t}_C^2 = 3.061 \cdot 10^4 \text{ s}^2$$

Convert t to θ_c by dividing each value by \bar{t}_c . Convert $c(t)$ to $C(\theta_c)$ by dividing each value by $\sum c_i \Delta t_i$ and multiplying with \bar{t}_c . Integrate $C(\theta_c)$ by using the mean values for each interval $\Delta\theta_c$ to get $F(t) = F(\theta_c)$ (Figure 3.3)

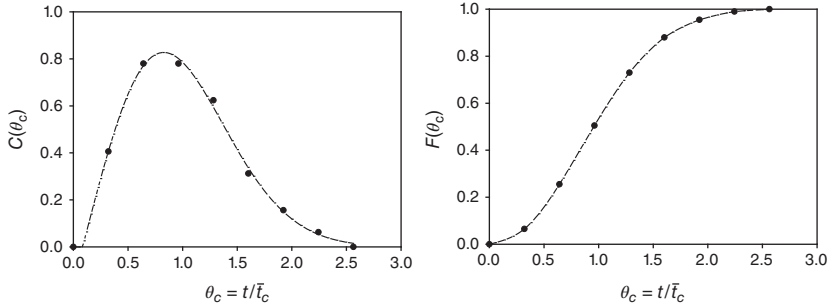


Figure 3.3 Experimental C- and F-curve as function of the dimensionless time.

3.3

RTD in Ideal Homogenous Reactors

Before we consider the RTD in real systems, we first examine the behavior of the ideal reactors presented in Chapter 2.

3.3.1

Ideal Plug Flow Reactor

The ideal plug flow reactor acts solely as a delaying element without changing the form of the input signal. In the case of an impulse function at the inlet, the same pulse function is obtained at the outlet after a time delay corresponding to the mean residence time \bar{t} .

$$E(t) = \delta(t - \bar{t}) \quad (3.25)$$

The same is true for the step function and its response $F(t)$.

3.3.2

Ideal Continuously Operated Stirred Tank Reactor (CSTR)

If the amount n_0 of a tracer is added in the form of a pulse to an ideally mixed stirred tank, the maximum concentration is established instantaneously

$$c_0 = \frac{n_0}{V}, \quad t = 0 \quad (3.26)$$

The concentration time course can then be predicted from the mass balance by integration

$$V \frac{dc(t)}{dt} = -\dot{V}c(t); \frac{dc(t)}{dt} = -\frac{\dot{V}}{V}c(t) = -\frac{1}{\bar{t}}c(t); \text{ constant density}$$

and

$$\frac{c(t)}{c_0} = \exp\left(-\frac{t}{\bar{t}}\right) = \exp(-\theta) = E(\theta) \quad (3.27)$$

With Equation 3.6 we obtain for the RTD:

$$E(t) = \frac{1}{\bar{t}}E(\theta) = \frac{1}{\bar{t}}\exp\left(-\frac{t}{\bar{t}}\right) \quad (3.28)$$

From this it follows by integration for the cumulative RTD (curve $F(t)$):

$$F(t) = \int_0^t E(t')dt' = 1 - \exp\left(-\frac{t}{\bar{t}}\right) \quad (3.29)$$

In Figures 3.4 and 3.5, the RTDs of ideal reactors are presented together with the RTD of a real reactor. The ideal, continuously operated stirred tank reactor (CSTR) has the broadest RTD between all reactor types. The most probable residence time for an entering volume element is $t=0$. After a mean residence time ($t = \bar{t}$), 37% of the tracer injected at time $t=0$ is still present in the reactor. After five mean residence times, a residue of about 1% still remains in the reactor. This means that at least five mean residence times must pass after a change in the inlet conditions before the CSTR effectively reaches its new stationary state.

3.3.3

Cascade of Ideal CSTR

The cascade consists of a series of ideal continuously operated stirred tank reactors, CSTR, connected one after the other. The outlet function of one CSTR is

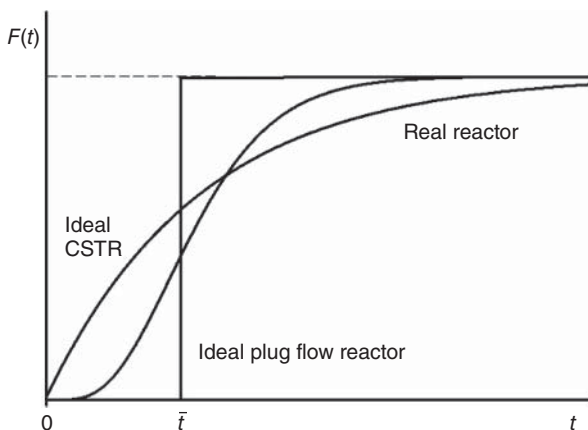


Figure 3.4 Cumulative RTD of ideal and real reactors.

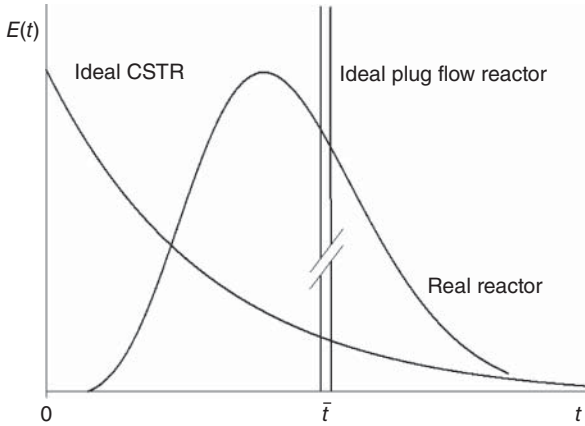


Figure 3.5 RTD curves of ideal and real reactors.

thus simultaneously the input function of the next one. As the transfer functions of each reactor are identical and known, the distribution function of a cascade of N tanks can be determined by successive convolution [4].

For a cascade of N tanks of equal space time τ_i we obtain for the RTD:

$$E(t) = \frac{1}{\bar{t}_i} \left(\frac{t}{\bar{t}_i} \right)^{N-1} \cdot \frac{1}{(N-1)!} \exp\left(-\frac{t}{\bar{t}_i}\right) \quad (3.30)$$

With $\bar{t} = N \cdot \bar{t}_i$ as mean residence time of the cascade:

$$\bar{t}E(t) = E = \frac{N(N \cdot \theta)^{N-1}}{(N-1)!} \exp(-N\theta) \quad (3.31)$$

The cumulative RTD curve can be calculated from this by integration.

$$F(t) = \int_0^t E(t') dt' = \frac{c(t)_N}{c_0} = 1 - \exp(-N\theta) \left[1 + N \cdot \theta + \frac{(N \cdot \theta)^2}{2!} + \dots + \frac{(N \cdot \theta)^{N-1}}{(N-1)!} \right] \quad (3.32)$$

The RTD of ideal cascades with different numbers of tanks in series are given in Figures 3.6 and 3.7. With increasing subdivision of the entire reactor volume into ideally mixed individual elements, the residence time becomes more and more uniform and the RTD curves become more symmetrical. The RTD of the cascade of the total volume V approaches that of an ideal plug flow reactor of the same volume and becomes identical with this when N goes toward infinity.

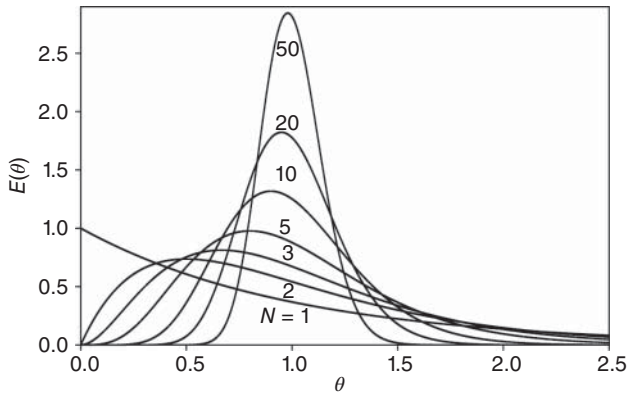


Figure 3.6 Residence time distribution in a cascade of stirred tanks, parameter: number of tanks. (Adapted from Ref. [4], Figure 4.20 Copyright © 2013, Wiley-VCH GmbH & Co. KGaA.)

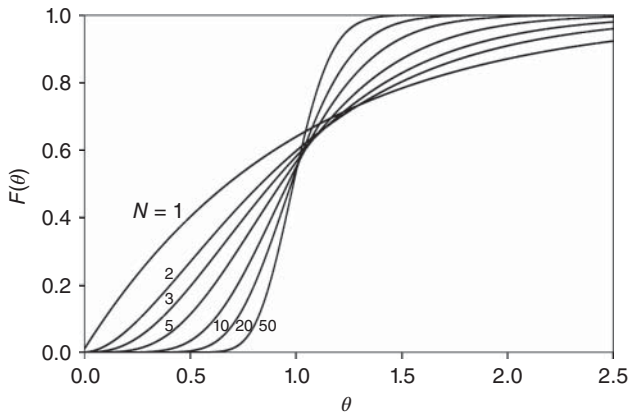


Figure 3.7 Cumulative residence time distribution curves of a cascade of stirred tanks, parameter: number of tanks. (Adapted from Ref. [4], Figure 6.30b Copyright © 2013, Wiley-VCH GmbH & Co. KGaA.)

3.4 RTD in Nonideal Homogeneous Reactors

3.4.1 Laminar Flow Tubular Reactors

Laminar flow is characterized by a parabolic velocity profile according to the Hagen–Poisuille law:

$$u(r) = u_{\max} \left(1 - \frac{r^2}{R^2} \right) = 2\bar{u}(1 - y^2); y = \frac{r}{R} = \frac{\text{radial distance}}{\text{tube radius}} \quad (3.33)$$

with u_{\max} , velocity in the center of the tube, and \bar{u} the average value over the cross section, which is equivalent to superficial velocity (u). If diffusion processes are neglected ($D_m = 0$), the residence time, which a volume element spends in the reactor, depends on its radial position in the tube.

$$t = \frac{L}{u} = \frac{L}{u_0(1-y^2)} = \frac{t_{\min}}{(1-y^2)} \quad (3.34)$$

With $t_{\min} = L/u_{\max}$ and $\bar{t} = 2 \cdot t_{\min}$

The fraction of the total liquid that is in the position y and thus has a residence time t can be deduced from the area of a circular ring with the radius R .

$$\frac{d\dot{V}}{\dot{V}} = \frac{u(r) \cdot 2\pi \cdot r \cdot dr}{\pi R^2 u} = \frac{2 \cdot u(r) \cdot r \cdot dr}{u \cdot R^2} = E(t)dt \quad (3.35)$$

With $t_{\min}/t = 1 - y^2$, it follows that

$$E(t)dt = \frac{2t_{\min}^2}{t^3} dt = \frac{\bar{t}^2}{2t^3} dt \quad (3.36)$$

and in dimensionless form

$$E = \tau \cdot E(t) = \bar{t} \cdot E(t) = 0.5\theta^{-3} \quad (3.37)$$

The F -curve is obtained by integration from t_{\min} to final time t

$$F = \int_{t_{\min}}^t E(t) dt = 1 - \left(\frac{\tau}{2t}\right)^2 = 1 - \left(\frac{\bar{t}}{2t}\right)^2 = 1 - \frac{1}{4\theta^2} \quad (3.38)$$

The RTD in laminar flow reactor without radial diffusion is shown in Figure 3.8. The first volume elements reach the reactor outlet after $\bar{t}/2$ ($\theta = 0.5$) and approaches zero slowly.

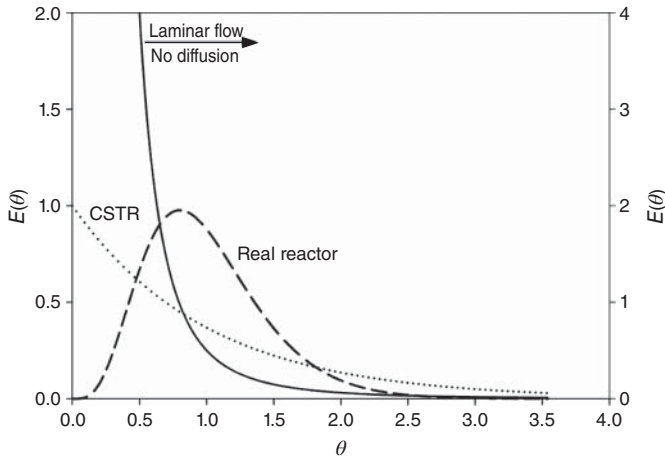


Figure 3.8 Residence time distribution in a laminar flow reactor (without radial diffusion).

3.4.2

RTD Models for Real Reactors

The experimental determination of the RTD in real reactors has two purposes: to characterize the reactor and to compare the behavior with that of an ideal system. Unwanted short-circuit flows or dead zones within a reactor can be recognized and can possibly be eliminated by constructional modifications. First of all, a real reactor is classified according to the degree of backmixing. The degree of backmixing is between that of the ideal plug flow reactor (no backmixing) and the ideal CSTR (complete backmixing). The proposed RTD model serves, in combination with the kinetic model, for the prediction of the reactor performance and the achievable selectivity and yield of the target product.

3.4.2.1 Tanks in Series Model

During the discussion of RTD in a cascade of identical ideal stirred tank reactors, we showed that the RTD becomes more narrow with the increasing number of tanks and that for N approaching infinity, the RTD corresponds to that of an ideal plug flow reactor. It is, therefore, possible to describe the RTD of a real system by the imaginary subdivision of the total volume into N identical, completely mixed cells as illustrated in Figure 3.9. As the degree of backmixing can be neglected outside the cascade, the tanks in series model can be applied only for systems closed for dispersion as shown in Figure 3.11b.

The RTD according to the cell model is described by Equation 3.39.

$$E(\theta) = E = \bar{t} \cdot E(t) = \frac{N(N \cdot \theta)^{N-1}}{(N-1)!} \exp(-N \cdot \theta), \quad \theta = t/\bar{t}$$

$$E(t) = \frac{1}{\bar{t}} \left(\frac{t}{\bar{t}} \right)^{N-1} \frac{N^N}{(N-1)!} \exp\left(-\frac{N \cdot t}{\bar{t}}\right) \quad (3.39)$$

The only model parameter is the number N of the cells in series, which can be determined by a direct fitting of the measured and calculated distribution curves or from the moments of the distribution. The main properties of the tanks in series model are presented in Figure 3.10.

The relationship between N and the variance according to the cell model is given by

$$\sigma_{\theta}^2 = \frac{1}{N} \quad (3.40)$$

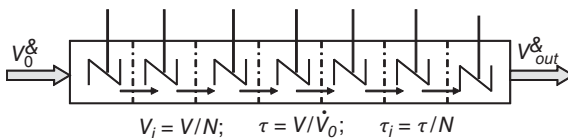


Figure 3.9 The tanks in series model (schematic).

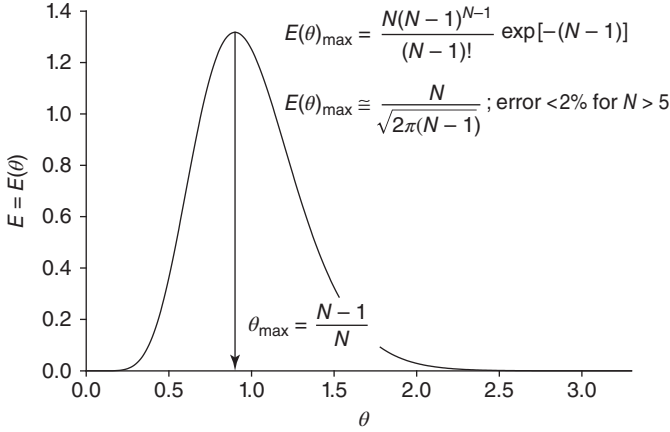


Figure 3.10 Properties of the RTD curve for the tanks in series model.

The mean residence time obtainable from the first moment of the distribution corresponds to the space time, if the density of the fluid is constant.

$$\bar{t} = \frac{V}{V_0} = \tau \quad (\rho = \text{constant}) \quad (3.41)$$

3.4.2.2 Dispersion Model

On the basis of an ideal plug flow reactor, a term considering the effective axial dispersion is added to the model. The axial dispersion does not take place solely through molecular diffusion, which is usually negligibly small, but mainly through deviations from ideal plug flow, caused by turbulent velocity variations and eddies. As all of these processes are linearly dependent on concentration gradients, they can be lumped together and treated in analogy to Fick's law. The axial dispersion processes is described with Equation 3.42.

$$J = -D_{\text{ax}} \frac{dc}{dz} \quad (3.42)$$

with D_{ax} as the axial dispersion coefficient.

The RTD as described by the dispersion model can be derived from the mass balance of a nonreacting species (tracer) over a volume element, $\Delta V = A_{\text{cs}} \Delta z$, where A_{cs} is the cross sectional area of the tube and z the axial coordinate. For constant fluid density and superficial velocity u , we obtain:

$$A_{\text{cs}} \Delta z \frac{\partial c}{\partial t} = u(c_z - c_{z+\Delta z}) A_{\text{cs}} + \left(-D_{\text{ax}} \frac{\partial c}{\partial z} \Big|_z + D_{\text{ax}} \frac{\partial c}{\partial z} \Big|_{z+\Delta z} \right) A_{\text{cs}}$$

and with $\Delta z \rightarrow 0$

$$\frac{\partial c}{\partial t} = -u \frac{\partial c}{\partial z} + D_{\text{ax}} \frac{\partial^2 c}{\partial z^2} \quad (3.43)$$

In dimensionless form Equation 3.43 becomes:

$$\frac{\partial C}{\partial \theta} = -\frac{\partial C}{\partial Z} + \frac{1}{Bo} \frac{\partial^2 C}{\partial Z^2} \quad (3.44)$$

with: $\theta = \frac{t}{\tau}$; $\tau = \frac{L}{u}$; $Z = \frac{z}{L}$; $C = \frac{c}{c_0}$; $\bar{c}_0 = \frac{n_0}{V_R}$; $Bo = \frac{uL}{D_{ax}}$

The total amount of a nonreactive tracer injected as a Dirac pulse at the reactor entrance is given by n_0 . The Bodenstein number, Bo , is defined as the ratio between the axial dispersion time, $t_{ax} = L^2/D_{ax}$, and the mean residence time, $\bar{t} = \tau = L/u$, which is identical to the space time for reaction mixtures with constant density. For $Bo \rightarrow 0$ the axial dispersion time is short compared to the mean residence time resulting in complete backmixing in the reactor. For $Bo \rightarrow \infty$ no dispersion occurs. In practice, axial dispersion can be neglected for $Bo \geq 100$.

To predict the response curve to an ideal pulse tracer injection at the entrance of the tubular reactor, the boundary conditions at both ends have to be known. Suppose the flow is undisturbed as it passes the inlet and the outlet boundaries of the reactor. This situation is depicted in Figure 3.11a and called an open/open system to dispersion. In contrary to this situation, ideal plug flow ($D_{ax} = 0$) is considered outside of the boundaries as illustrated in Figure 3.11b. A sudden change of the axial dispersion occurs at the inlet and the outlet of the reactor. This situation corresponds to a closed/closed system. In addition to these situations, vessels open for dispersion at only one site can be discussed.

Only for an open/open system, an analytical expression exists to describe the experimental response on a tracer pulse at the reactor inlet. The C -curve (see Equation 3.27) is given in Equation 3.45 as function of the dimensionless time.

$$C(\theta_c) = \frac{1}{2} \sqrt{\frac{Bo}{\pi\theta_c}} \exp\left(\frac{-(1-\theta_c)^2 Bo}{4\theta_c}\right); \text{ open/open system} \quad (3.45)$$

with $\theta_c = t/\bar{t}_c$.

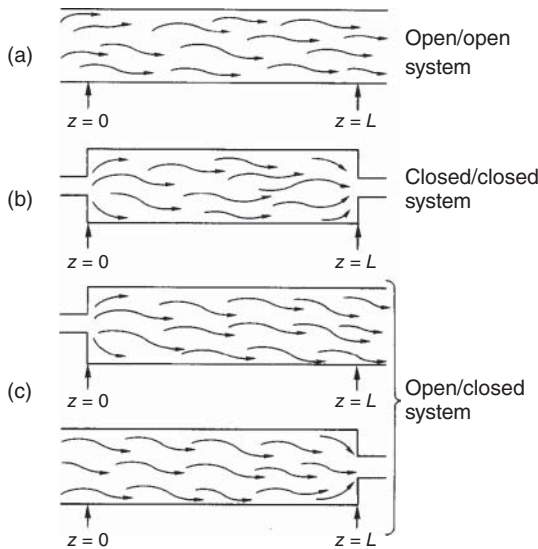


Figure 3.11 (a–c) Boundary conditions for a tubular reactor.

The relation between the mean value of the measured distribution curve compared to the mean of the E -curve, respectively, the space time for constant density is given in Equation 3.46:

$$\bar{\theta}_c = \frac{\bar{t}_c}{\tau} = \frac{\bar{t}_c}{\bar{t}} = 1 + \frac{2}{Bo} \quad (\text{constant density}) \quad (3.46)$$

The variance of the distribution $E(t)$ is given by:

$$\sigma_\theta^2 = \frac{\sigma_c^2}{\tau^2} = \frac{\sigma_c^2}{\bar{t}^2} = \frac{2}{Bo} + \frac{8}{Bo^2} \quad (3.47)$$

Replacing \bar{t} by the mean value from the experimental curve leads to (Example 3.2):

$$\bar{t} = \frac{\bar{t}_c}{(1 + 2/Bo)}; \Rightarrow \frac{\sigma_c^2}{\bar{t}^2} = \sigma_{\theta_c}^2 = \frac{2/Bo + 8/Bo^2}{(1 + 2/Bo)^2} \quad (3.48)$$

The predicted response curves to tracer pulse are shown in Figure 3.12 for different values of the Bo . In contrast to the C -curves, E -curves are experimentally not directly measurable. For the open/open boundary conditions follow [5]:

$$E(\theta) = \frac{1}{2\theta} \sqrt{\frac{Bo}{\pi\theta}} \exp\left(\frac{-(1-\theta)^2 Bo}{4\theta}\right); \quad \text{open/open system} \quad (3.49)$$

With decreasing dispersion, increasing values of Bo , the distribution curves become more and more symmetric and for $Bo \geq 100$ a Gaussian distribution results with

$$C(\theta) = E(\theta) = \frac{1}{2} \sqrt{\frac{Bo}{\pi}} \exp\left(\frac{-(1-\theta)^2 Bo}{4\theta}\right); \quad Bo \geq 100 \quad (3.50)$$

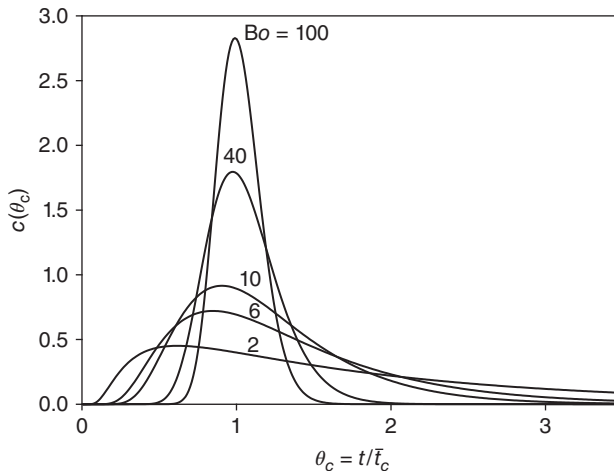


Figure 3.12 Residence time distribution according to the dispersion model. (Adapted from Ref. [6], Figure 27.23 Copyright © 2012, Wiley-VCH GmbH & Co. KGaA.)

Mean and variance are given by the following simple relations:

$$\begin{aligned}\bar{\theta} &= \frac{\bar{t}}{\tau} = 1 \\ \sigma_{\theta}^2 &= \frac{\sigma^2}{\tau^2} = \frac{2}{Bo} \quad Bo \geq 100, \rho = \text{const}\end{aligned}\quad (3.51)$$

In addition, the distribution curves calculated by the dispersion and the cell models coincide, and the following equivalence between the model parameters results.

$$N \approx \frac{Bo}{2} \quad (3.52)$$

For *closed/closed* and *closed/open* vessels, analytical expressions for calculating the response curves are not available. But the mean and the variance of the distribution can be calculated with the following relations:

- *Closed/closed system, constant density*

$$\begin{aligned}\bar{\theta} &= \bar{t}/\tau = 1 \\ \sigma_{\theta}^2 &= \frac{\sigma^2}{\tau^2} = \frac{2}{Bo} - \frac{2}{Bo^2}(1 - \exp(-Bo))\end{aligned}\quad (3.53)$$

- *Open/closed system, constant density*

$$\begin{aligned}\bar{\theta}_c &= \frac{\bar{t}_c}{\tau} = \frac{\bar{t}_c}{t} = 1 + \frac{1}{Bo} \\ \sigma_{\theta}^2 &= \frac{\sigma_c^2}{\tau^2} = \frac{\sigma_c^2}{t^2} = \frac{2}{Bo} + \frac{3}{Bo^2}\end{aligned}\quad (3.54)$$

To avoid errors because of the nonideal inlet pulses, the injected tracer can be measured at the reactor inlet and outlet. The model parameter can be obtained by the convolution of the inlet signal, $g(t)_{\text{in}}$, with the RTD function and parameter fitting.

$$g(t)_{\text{out}} = g(t)_{\text{in}} \cdot E(t) \quad (3.55)$$

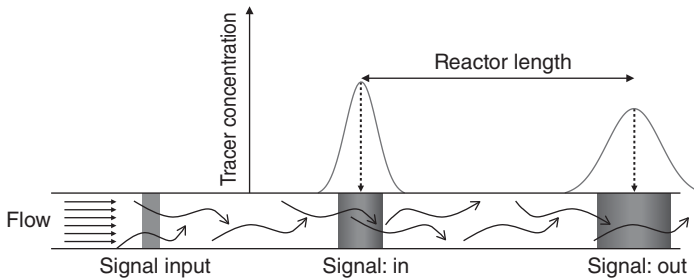


Figure 3.13 RTD characteristics from two measurements (open/open system). (Adapted from Ref. [6], Figure 27.24 Copyright © 2012, Wiley-VCH GmbH & Co. KGaA.)

The additive property of variances also allows to treat any measured tracer pulse input and to extract from it the mean residence time and the variance of the measured outlet curve as indicated in Figure 3.13 and Equation 3.56.

$$\begin{aligned}\Delta \bar{t} &= \bar{t}_{\text{out}} - \bar{t}_{\text{in}} \\ \Delta \sigma^2 &= \sigma_{\text{out}}^2 - \sigma_{\text{in}}^2 \\ \frac{\Delta \sigma^2}{\Delta \bar{t}^2} &= \Delta \sigma_{\theta}^2 = \frac{2}{Bo}\end{aligned}\quad (3.56)$$

Example 3.2: Estimation of Bo -number from measured response curves.

On the basis of the experimental results presented in Example 3.1, estimate the Bo supposing that the tubular reactor can be considered as (a) a system closed for dispersion and (b) open for dispersion on both sides.

- 1) For a closed system experimental mean residence time corresponds to the real residence time in the reactor and, for constant density of the fluid, to the space time (Equation 3.53): $\bar{t}_c = \bar{t} = \tau$. The Bo can be calculated with Equation 3.53:

$$\begin{aligned}\frac{\sigma_c^2}{\bar{t}_c^2} &= \frac{\sigma^2}{\bar{t}^2} = \frac{\sigma^2}{\tau^2} = \sigma_{\theta}^2 = \frac{2}{Bo} - \frac{2}{Bo^2}(1 - \exp(-Bo)) \\ \text{with } \frac{\sigma_c^2}{\bar{t}_c^2} &= \frac{34,208.6}{(374.4)^2} = 0.2184\end{aligned}$$

Bo can be estimated by trial-and-error or by using an equation solver:
 $Bo = 8.0$

- 2) For an open/open system we found the following relationship between \bar{t}_c and \bar{t} (Equation 3.48): $\bar{t} = \tau = \frac{\bar{t}_c}{(1+2/Bo)}$ constant density. The Bo can be obtained from: $\frac{\sigma_c^2}{\bar{t}_c^2} = 0.2184 = \frac{2/Bo+8/Bo^2}{(1+2/Bo)^2}$. Estimation with an equation solver results in $Bo = 8.85$ and $\bar{t} = \tau = \frac{374.4}{1+2/8.85} = 305.4$ s.

3.4.3

Estimation of RTD in Tubular Reactors

For the design of tubular reactors an *a priori* estimation of the axial dispersion is indispensable. The dispersion in tubular reactors depends on the flow regime, characterized by the Reynolds number, Re , and the physical properties of the fluid, characterized by the Schmidt number, Sc . In addition, the presence of internal packings influences the flow behavior and, in consequence, the axial dispersion of the fluid.

In the literature, a large number of experimental data are available correlating the axial Péclet number (Pe) with the Re and Sc . The axial Pe has as characteristic parameter the diameter d_t in tubular reactors, or the particle diameter d_p in packed bed reactors.

$$Pe_{ax} = \frac{u \cdot d_t}{D_{ax}} \text{ (tube)} \quad Pe_{ax} = \frac{u \cdot d_p}{\varepsilon_{bed} \cdot D_{ax}} \text{ (packed bed); } u : \text{ superficial velocity} \quad (3.57)$$

The relation between the Bo characterizing the dispersion in the chemical reactor and the Pe becomes:

$$Bo = Pe_{ax} \frac{L}{d_t} \quad (3.58)$$

Correlations between Pe_{ax} and Re , respectively $Re \cdot Sc$, are summarized in Table 3.2 together with the definitions of the model parameters. The presented correlations are compared with experimental results, indicated as gray area, in Figures 3.14 and 3.15.

In general, axial dispersion decreases with increasing values for Re and $Re \cdot Sc$. An exception is the behavior of empty tubes under laminar flow conditions. For laminar flow a parabolic velocity profile develops. Under these conditions, molecular diffusion in axial and radial directions plays an important role in RTD. The diffusion in the radial direction tends to diminish the spreading effect of the parabolic velocity profile, while in the axial direction the molecular diffusion increases the dispersion. As a result the axial dispersion passes through a minimum (Pe_{ax} passes through a maximum) as function of $Re \cdot Sc = u \cdot d_t / D_m$ at $Re \cdot Sc = \sqrt{\chi}$ (see Equation 3.59).

Table 3.2 Estimation of axial dispersion in tubular reactors [6].

Definitions: $Pe_{ax} = \frac{u \cdot d_p}{\varepsilon_{bed} \cdot D_{ax}}$; $Re_p = \frac{u \cdot d_p}{\nu}$; $d_p = 6 \frac{V_p}{A_p}$; $Re = \frac{u \cdot d_t}{\nu}$; $Sc = \frac{\nu}{D_m}$;

Empty tube, laminar flow:

$$D_{ax} = D_m + \chi \frac{u^2 d_t^2}{D_m} \quad \frac{1}{Pe_{ax}} = \frac{1}{Re \cdot Sc} + \frac{Re \cdot Sc}{\chi} \cdot \frac{L}{d_t} > 0.04 \frac{u \cdot d_t}{D_m}; \chi = \frac{1}{192} \text{ for circular tubes} \quad (3.59)$$

Empty tube, turbulent flow:

$$\frac{1}{Pe_{ax}} = \frac{3 \cdot 10^7}{Re^{2.1}} + \frac{1.35}{Re^{1/8}}; Pe_{ax} = \frac{u \cdot d_t}{D_{ax}} \quad (3.60)$$

Packed bed, gas flow:

$$\frac{1}{Pe_{ax}} = \frac{0.3}{Re_p \cdot Sc} + \frac{0.5}{1 + \frac{3.8}{Re_p \cdot Sc}}; \frac{d_t}{d_p} > 15; 0.008 < Re_p < 400 \quad (3.61)$$

$0.28 < Sc < 2.2$

Packed bed, liquid flow:

$$\varepsilon_{bed} \cdot Pe_{ax} = 0.2 + 0.011 \cdot Re_p^{0.48}; \frac{d_p}{d_t} > 15; 10^{-3} < Re_p < 10^3 \quad (3.62)$$

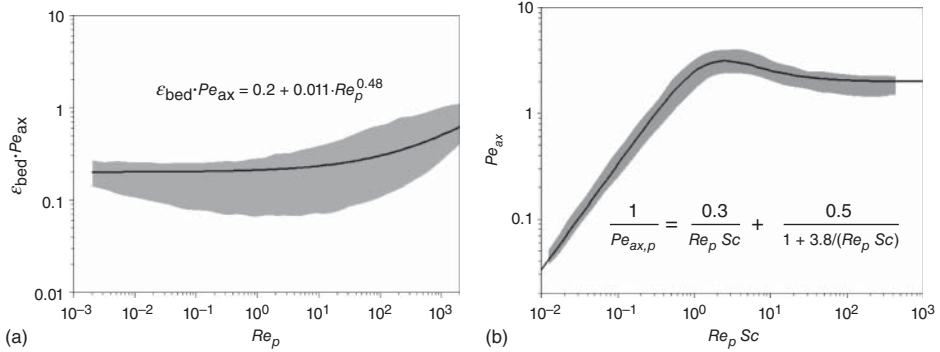


Figure 3.14 Axial dispersion in fixed-bed reactors: (a) liquid flow and (b) gas flow [6]. Gray area represents experimental results. (Adapted from [6], Figure 27.24 Copyright © 2012, Wiley-VCH GmbH & Co. KGaA.)

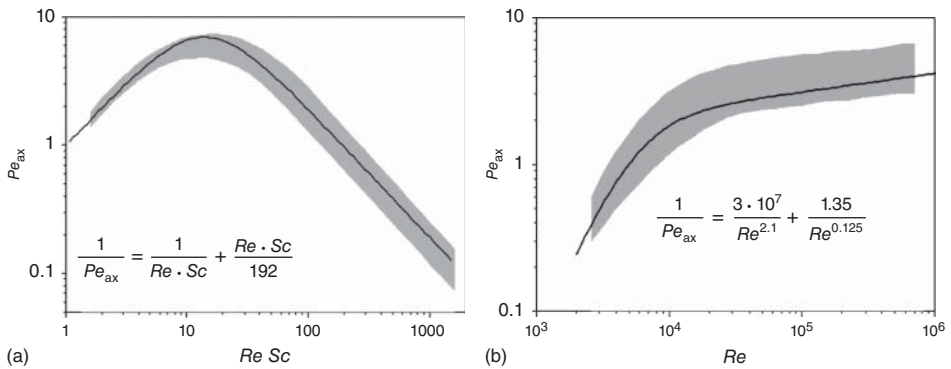


Figure 3.15 Axial dispersion in tubular reactors: (a) laminar flow and (b) turbulent flow. Gray area represents experimental results. (Adapted from [6], Figure 27.25 Copyright © 2012, Wiley-VCH GmbH & Co. KGaA.)

3.5 Influence of RTD on the Reactor Performance

For reactions with positive reaction order, the reactor performance will decrease with the broadening of the RTD at constant mean residence time. This can easily be demonstrated with Figure 3.16, where the conversion obtained in an ideal plug flow reactor is plotted as function of the residence time. For a residence time of 15 min the conversion in the ideal tubular reactor corresponds to $X = 0.78$ (point A in Figure 3.16). Supposing the fluid is distributed in two equal parts in plug flow reactors with residence times of 5 and 25 min, resulting in the same mean residence time of 15 min. The corresponding conversions obtained are 0.39 (point B_1) and 0.92 (point B_2). The mean conversion is indicated by point M on the line relating B_1 and B_2 . The mean conversion dropped to $X = 0.66$ as a result of the

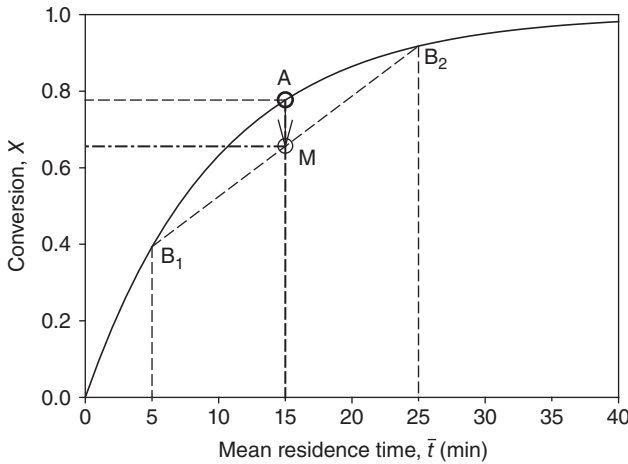


Figure 3.16 Influence of RTD on the performance of tubular reactors. First order reaction, $k = 0.1 \text{ min}^{-1}$.

RTD. The result can be generalized: RTD will diminish the conversion and the specific reactor performance for reactions with a positive reaction order ($n > 0$).

3.5.1

Performance Estimation Based on Measured RTD

In the case of known formal kinetics, the reactor performance can be determined directly from the RTD. We can imagine, for example, that the RTD in the reactor under consideration can be represented by a series of ideal plug flow reactors of different lengths arranged in parallel through which the reaction mass flows at equal rates (see Figure 3.17).

The conversion at the end of an individual tube with a defined residence time can then be calculated easily. At the exit of the tubes, the various flows having different residence times are mixed; the result is an average conversion or, respectively, an average reactant concentration. When RTD and kinetics are known, it follows that:

$$\left\{ \begin{array}{l} \text{average conversion} \\ \text{at reactor outlet} \end{array} \right\} = \sum \left\{ \begin{array}{l} \text{conversion in} \\ \text{volume element} \\ \text{with residence time } t_i \end{array} \right\} \cdot \left\{ \begin{array}{l} \text{fraction of} \\ \text{total flow with} \\ \text{residence time } t_i \end{array} \right\} \quad (3.63)$$

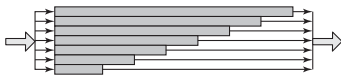


Figure 3.17 Real reactor behavior modeled by ideal tubular reactors arranged in parallel.

$$\bar{X} = \int_0^1 X(t) \cdot dF \cong \sum_0^1 X(t_i) \cdot \Delta F_i$$

or with $dF = E(t)dt$

$$\bar{X} = \int_0^\infty X(t) \cdot E(t)dt \cong \sum_0^\infty X(t_i) \cdot E(t_i)\Delta t_i \quad (3.64)$$

The presented method leads to exact values only for first order reaction (demonstrated in Examples 3.3–3.5) or for reactions in completely segregated systems (see Chapter 4). But, the proposed methods can be used also for a good estimation of reactor performances for reactions with $n \neq 1$.

Example 3.3: Estimation of conversion in real reactors.

Estimate the conversion for the first order reaction in a nonideal tubular flow reactor. The residence time distribution is characterized by measured F function. The mean residence time can be calculated with Equation 3.14 applying the trapezoidal method. Compare the result with the conversion that could be obtained in ideal PFR and CSTR for the same mean residence of 10 min. $-R_1 = k \cdot c_1$; $k = 0.15 \text{ min}^{-1}$

Solution:

- 1) In Figure 3.18 the conversion is plotted as function of $F(t)$ with values of Table 3.3. The mean conversion is obtained estimating the area under the X - F -curve. Numerical integration using the trapezoidal method results in

$$\bar{X} = \sum_0^1 X(t) \cdot \Delta F_i = 0.72$$

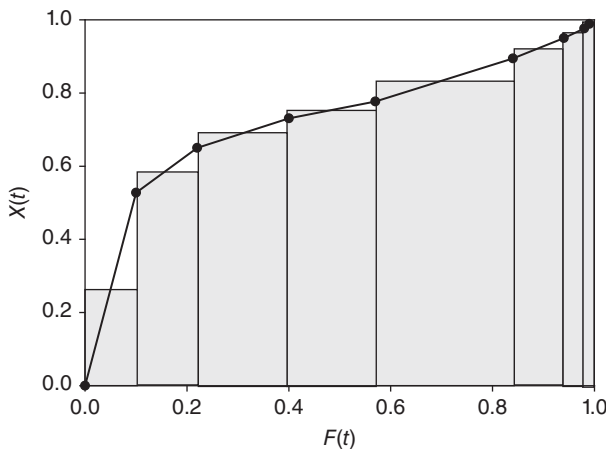


Figure 3.18 Conversion as a function of $F(t)$.

2) Ideal plug flow reactor:

$$X = 1 - \exp(-k \cdot \tau) = X = 1 - \exp(-0.15 \cdot 10) = 0.777$$

3) Continuous stirred tank reactor:

$$X = \frac{k \cdot \tau}{1 + k \cdot \tau} = \frac{0.15 \cdot 10}{1 + 0.15 \cdot 10} = 0.6$$

Table 3.3 Residence time of a tubular reactor.

t (min)	0	5	7	8.75	10	15	20	25	30
F [-]	0	0.10	0.22	0.40	0.57	0.84	0.94	0.98	0.99
X [-]	0	0.394	0.503	0.583	0.632	0.777	0.865	0.918	0.950

Example 3.4: Conversion in laminar flow tubular reactors.

Estimate the conversion obtainable in a tubular reactor under laminar flow conditions neglecting radial diffusion for the reaction presented in Example 3.3. The mean residence time is $\bar{t} = 10$ min.

Solution:

The RTD in laminar flow reactors is given in Equations 3.36 and 3.38.

$$E(t)dt = \frac{\bar{t}^2}{2t^3} dt;$$

$$F = \int_{t_{\min}}^{t'} E(t)dt = 1 - \left(\frac{\bar{t}}{2t}\right)^2$$

With Equation 3.64 we obtain:

$$\bar{X} = \int_0^{\infty} X(t) \cdot E(t)dt = \int_0^{\infty} (1 - \exp(-k \cdot t)) \cdot \frac{\bar{t}^2}{2t^3} dt$$

Numerical integration between $0 < t < 100$ min leads to a mean conversion of $\bar{X} = 0.69$.

3.5.2

Performance Estimation Based on RTD Models

In the case of identical mean residence times for different tubular reactors, the conversion and selectivity of a complex reaction will depend on the RTD in the reactor. With increasing backmixing, the reactor approaches the behavior of an ideal CSTR. Accordingly, the performance of any tubular reactor will decrease with increasing RTD at a constant mean residence time for reactions with formally positive reaction orders.

3.5.2.1 Dispersion Model

Backmixing in a tubular reactor has a direct influence on the axial concentration profile. With decreasing axial dispersion time compared to the space time (decreasing Bo) the concentration profile flattens and finally a uniform concentration results ($Bo \Rightarrow 0$). This is demonstrated in Figure 3.19 for an irreversible first order reaction at $DaI = k \cdot \tau = 3$.

For reactions with positive reaction order, the flattening of concentration profile diminishes the mean reaction rate in the tubular reactor and the conversion will decrease at constant space time, constant DaI , respectively.

On the basis of the dispersion model, the following mass balance for a small volume element results:

$$u \frac{dc_1}{dz} - D_{ax} \frac{d^2c_1}{dz^2} - R_1 = 0 \quad (3.65)$$

or, respectively, in dimensionless form:

$$-\frac{dX}{dZ} - \frac{\tau(R_1)}{c_{1,0}} + \frac{D_{ax}}{u \cdot L} \frac{d^2X}{dZ^2} = 0 \quad (3.66)$$

Applying Danckwerts' boundary conditions [2] Equation 3.66 can be solved for an irreversible first order reaction (Equation 3.67) [6].

$$1 - X = \frac{4a \exp(Bo/2)}{(1+a)^2 \exp(aBo/2) - (1-a)^2 \exp(-aBo/2)}$$

with $a = \sqrt{1 + 4DaI/Bo}$ (3.67)

The conversion is a function of DaI and the axial dispersion characterized by Bo as shown in Figure 3.20. With decreasing Bo the conversion diminishes at constant DaI (constant space time). At $DaI = 5$ a conversion of $X = 0.99$ is attained in a plug flow reactor ($Bo = \infty$), whereas the conversion drops to $X = 0.83$ for $Bo = 0$ (continuous stirred tank reactor).

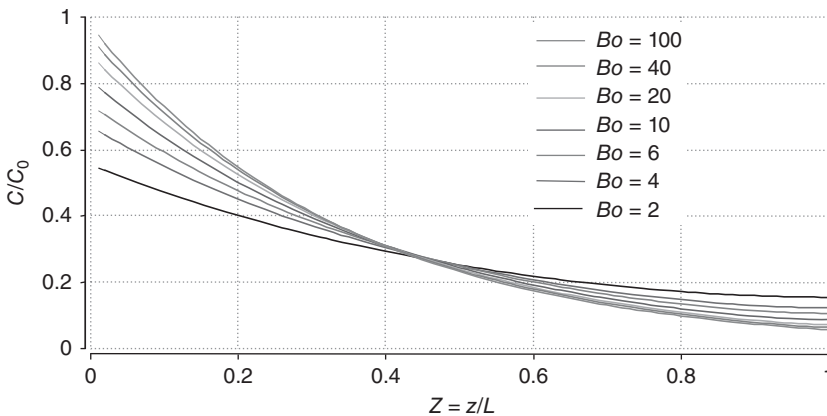


Figure 3.19 Influence of Bo on the axial concentration profile. First order reaction, $DaI = 3$. (Adapted from Ref. [6], Figure 27.26 Copyright © 2012, Wiley-VCH GmbH & Co. KGaA.)

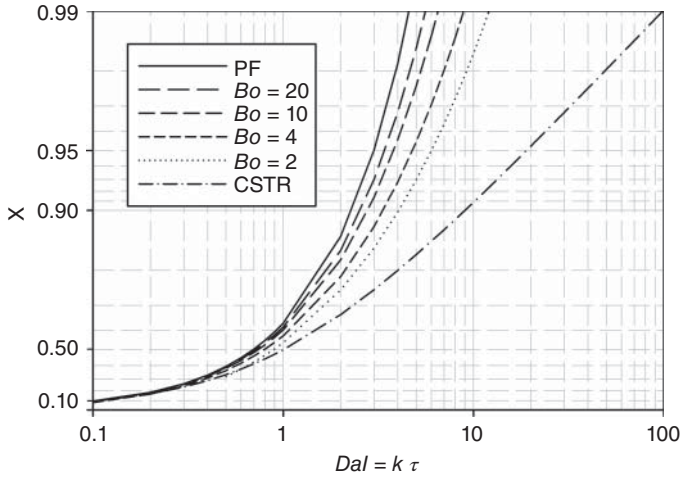


Figure 3.20 Conversion as function of Dal and Bo (first order reaction).

3.5.2.2 Tanks in Series Model

In Section 3.4.2, it was shown that the RTD in real reactors can be described with a series of ideally continuous stirred tank reactors. The scheme of such a cascade of continuous stirred tanks is shown in Figure 3.21. The total volume is divided in N equal sized stirred vessels.

For reactions with positive order, the performance of such a cascade reactor has a specific function between an ideal plug flow reactor and a single CSTR. This can easily be understood comparing the reactant concentration as function of the reactor volume. In a PFR the concentration and, therefore, the transformation rate diminishes with increasing volume from the reactor entrance to the outlet. The low specific performance of a CSTR can be explained by the overall low concentration corresponding to the outlet concentration. In the cascade, the concentration diminishes stepwise from one vessel to the next. This is shown schematically for a series with $N = 5$ vessel in Figure 3.22. With increasing number of equal sized vessels the concentration profile approaches that of a PFR.

The conversion in each vessel can be determined with the material balance for continuous ideally mixed vessels (see Section 2.2.3).

$$\dot{V}_0 c_{1,0} - \dot{V}_{\text{out}} c_{1,\text{out}} = V(-R_1) \text{ (steady state)} \tag{3.68}$$

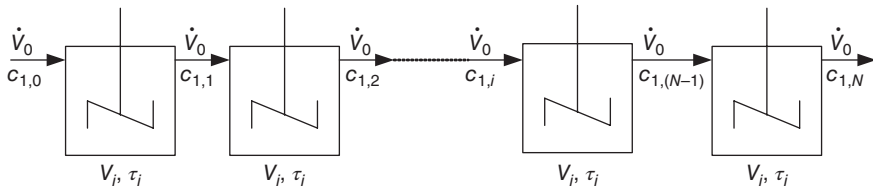


Figure 3.21 Cascade of continuous stirred tank reactors.

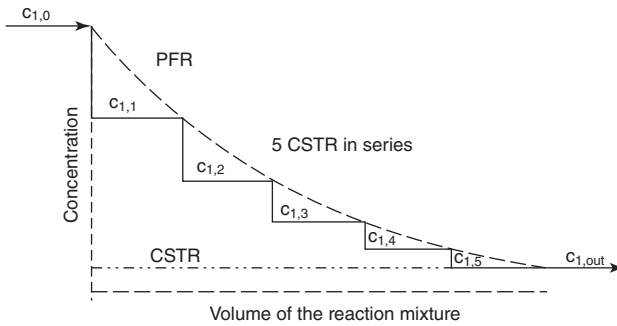


Figure 3.22 Concentration profile in a cascade with five stages in comparison with a PFR and a single CSTR.

Supposing an irreversible first order reaction and constant fluid density ($\alpha = 0$), we get for the first vessel:

$$\begin{aligned} \dot{V}_0(c_{1,0} - c_{1,1}) &= V_1 \cdot k c_{1,1}; \quad c_{1,0} - c_{1,1} = \frac{V_1}{\dot{V}_0} \cdot k c_{1,1} \\ \frac{c_{1,1}}{c_{1,0}} &= \frac{1}{1 + k\tau_1} \end{aligned} \quad (3.69)$$

The outlet concentration of the first vessel corresponds to the inlet concentration of the second one. We finally find:

$$\frac{c_{1,1}}{c_{1,0}} = \frac{c_{1,2}}{c_{1,1}} = \frac{c_{1,3}}{c_{1,2}} = \frac{c_{1,i}}{c_{1,i-1}} \dots = \frac{c_{1,N}}{c_{1,N-1}} = \frac{1}{1 + k\tau_i}; \quad \tau_1 = \tau_2 = \dots = \tau_i = \frac{\tau}{N} \quad (3.70)$$

$$\frac{c_{1,N}}{c_{1,0}} = 1 - X = \frac{1}{(1 + k\tau/N)^N} = \frac{1}{(1 + DaI/N)^N} \quad (3.71)$$

In Figure 3.23 the unreacted fraction of the key reactant ($f_1 = 1 - X$) is plotted against the Damköhler number for different stirred tanks in series. For $N \rightarrow \infty$ the final conversion corresponds to that of an ideal PFR.

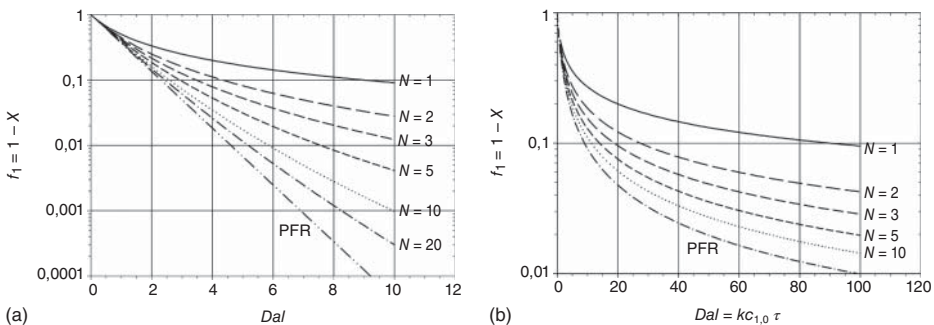


Figure 3.23 Unreacted fraction as function of Dal and N : (a) first order reaction and (b) second order reaction.

Example 3.5: Estimation of conversion based on RTD-models.

A first order reaction is carried out in the real reactor with an RTD characterized in Examples 3.1 and 3.2. Under reaction conditions the rate constant is found to be $k = 2.67 \cdot 10^{-3} \text{ s}^{-1}$. Estimate the conversion based on the kinetics and the experimental RTD and compare the results with predictions based on the cell-in-series and the dispersion model.

Solution:

Following the model of parallel arranged plug flow reactors, the mean conversion in a real reactor can be estimated with Equation 3.64

$$\bar{X} = \int_0^{\infty} X(t) \cdot E(t) dt \cong \sum X(t_i) \cdot E(t_i) \Delta t_i$$

In Example 3.1 we calculated $C(\theta)$ and plotted it in Figure 3.3. To apply Equation 3.64 we have to multiply $C(\theta)$ with the mean residence time and to calculate the conversion as function of time with the given kinetics. We suppose a closed/closed system. Thus $C(t) = E(t)$. The result is shown in the following table:

T (s)	0	120	240	360	480	600	720	840	960
$E(t) \cdot 10^3$	0	1.083	2.083	2.083	1.667	0.833	0.417	0.167	0
$X(t)$	0	0.274	0.473	0.618	0.722	0.799	0.854	0.894	0.923

Applying Equation 3.64 results in $\bar{X} = 0.59$.

For a first order reaction the conversion can be calculated with the *dispersion model* (Equation 3.67). As the model supposes a closed/closed system, we obtain with $Bo = 8$ and $\bar{t} = 374.4 \text{ s} \Rightarrow DaI = 2.67 \cdot 10^{-3} \cdot 374.4 = 1; \bar{X} = 0.60$.

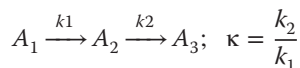
For the *tanks in series model* we estimate the number of cells with the Bo :

$N \cong Bo/2 = 4$. Applying Equation 3.71 for $N = 4$ tanks in series we obtain with $DaI = 1$:

$$f_{1,N} = 1 - \bar{X} = \frac{1}{\left(1 + \frac{k\tau}{N}\right)^N} = \frac{1}{\left(1 + \frac{1}{3.5}\right)^{3.5}} = 0.415; \bar{X} = 0.59$$

The results demonstrate that the predicted mean conversion can be calculated with one of the discussed methods giving roughly identical results.

In complex reaction systems, axial dispersion will also affect the product yield and selectivity attainable in real tubular reactors. This will be demonstrated for first order consecutive reactions.



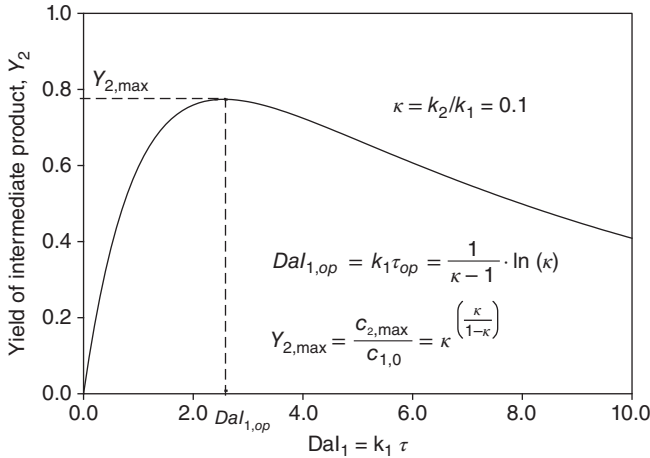


Figure 3.24 First order consecutive reactions. Yield of the intermediate as function of space time.

The yield of the intermediate product $Y_2 = \frac{c_2}{c_{1,0}}$ depends on the space time and the ratio of the rate constants, κ . It follows with Da_{l_1} , the Damköhler number referred to the first reaction (Figure 3.24):

$$Y_2 = \frac{1}{\kappa - 1} [\exp(-Da_{l_1}) - \exp(-\kappa Da_{l_1})] \quad (3.72)$$

The product yield first increases up to a maximum value ($Y_{2,max}$) and falls down to zero for $Da_{l_1} \Rightarrow \infty$. The maximum is attained at the optimal time, respectively, Da -number $Da_{l_1,op}$. At higher or lower values the yield diminishes. Therefore, it is evident that the highest yield can be reached only in an ideal plug flow reactor with a space time corresponding to $Da_{l_1,op}$. Any RTD in real tubular reactors will never allow the maximum yield of the intermediate. This is demonstrated for three different values of $\kappa = k_2/k_1$ in Figure 3.25. The real tubular reactor is modeled with the cell model.

3.6

RTD in Microchannel Reactors

Flow in microchannels with diameters between 10 and 1000 μm is mostly laminar and has a parabolic velocity profile. Therefore, the molecular diffusion in axial and radial directions plays an important role in RTD. The diffusion in the radial direction tends to diminish the spreading effect of the parabolic velocity profile, while in the axial direction the molecular diffusion increases the dispersion [7, 8]. With the so-called Taylor-Aris correlation the axial dispersion coefficient can be predicted based on the molecular diffusion coefficient D_m , the mean velocity of the stratified flow, the hydraulic diameter of the microchannel, and the geometry

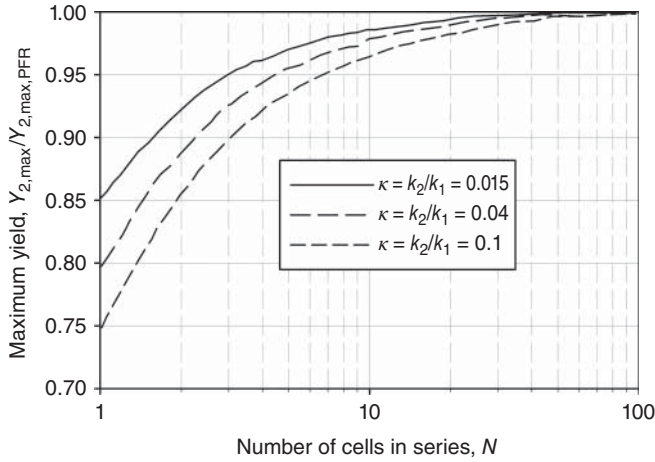


Figure 3.25 Maximum yield of intermediate product referred to maximum yield in PFR as function of axial dispersion (cell model).

of the cross section:

$$D_{ax} = D_m + \chi \cdot \frac{u^2 d_h^2}{D_m} \quad (3.73)$$

with $\chi = 1/119$ for square and $\chi = 1/192$ for circular cross section.

The dispersion in tubular reactors can be estimated for stratified flow in microchannels by introducing Equation 3.73 in the Bo -number.

$$\frac{1}{Bo} = \frac{D_{ax}}{\bar{u} \cdot L} = \frac{D_m L}{\tau^{1/2} \frac{u}{D_m}} + \chi \frac{d_h^2 u}{t_{D,rad} \tau} \quad (3.74)$$

The first term in Equation 3.74 corresponds to the ratio between space time and characteristic axial molecular diffusion time ($t_{D,ax} = L^2/D_m$). The second term corresponds to the ratio between radial diffusion time and space time. Molecular diffusion coefficients are in the order of $10^{-5} \text{ m}^2 \text{ s}^{-1}$ for gases and $10^{-9} \text{ m}^2 \text{ s}^{-1}$ for liquids. For microchannels with the length of several centimeter and mean residence times of seconds, axial diffusion can be neglected. In consequence, the dispersion in the channel is determined mainly by the ratio between the mean residence time in the reactor and the characteristic radial diffusion time. It follows:

$$\begin{aligned} Bo &\cong \frac{1}{\chi} \cdot \frac{D_m}{d_h^2} \cdot \frac{L}{u}; \\ Bo &\cong 192 \cdot \frac{D_m}{d_t^2} \cdot \frac{L}{u} = 48 \frac{\tau}{t_{D,rad}}, \text{ circular tube} \\ Bo &\cong 119 \cdot \frac{D_m}{d_h^2} \cdot \frac{L}{u} = 30 \frac{\tau}{t_{D,rad}}, \text{ square channels} \end{aligned} \quad (3.75)$$

3.6.1

RTD of Gas Flow in Microchannels

Axial dispersion can be neglected ($Bo \geq 100$), if the space time is at least two times the radial diffusion time. Accordingly, axial dispersion of gases in microchannels can be neglected, if their diameters are less than 1000 μm and the space time is longer than 0.1 s. This could also be proved experimentally.

The approach can also be used for multichannel reactors. Because of the small volume of a single channel, many channels have to be used in parallel to obtain sufficient reactor throughput. A uniform distribution of the reaction mixture over thousands of microchannels is necessary to obtain an adequate performance of the microstructured reactor. Flow maldistribution will enlarge the RTD in the multi-tubular reactor and lead to a reduced reactor performance along with reduced product yield and selectivity. Therefore, several authors have presented design studies of flow distribution manifolds [9–13].

Besides maldistribution, small deviations in the channel diameter introduced during the manufacturing process cause an enlargement of the RTD. The deviations may also be because of a nonuniform coating of the channel walls with catalytic layers. If the number of parallel channels is large ($N > 30$), a normal distribution of the channel diameters with a standard deviation σ can be assumed. The relative standard deviation, $\hat{\sigma}_d = \sigma_d / \bar{d}_i$ influences the pressure drop over the micro-reactor [11]:

$$\Delta p = \frac{128 \cdot \eta \cdot \dot{V}_{\text{tot}} \cdot L}{\pi \cdot N \cdot \bar{d}_i^4 \cdot (1 + 6\hat{\sigma}_d^2)} \quad (3.76)$$

The relation (3.76) shows that a variation of the channel diameter leads to a decrease of the pressure drop at a constant overall volumetric flow. As the pressure drop for each channel is identical, the variation of the diameter results in a variation of the individual flow rates, \dot{V}_i ; and the residence time, $\tau_i = V_i / \dot{V}_i$.

Supposing plug flow in each channel ($Bo_i \rightarrow \infty$), the overall dispersion is inversely proportional to the relative standard deviation and can be estimated by Equation 3.77 [11]:

$$Bo_{\text{reactor}} \cong \frac{d_i^2}{2\sigma_d^2} \quad (3.77)$$

In consequence, the plug flow behavior in a multichannel micro-reactor ($Bo_{\text{reactor}} \geq 100$) can be assumed only if the relative standard deviation is $\frac{\sigma_d}{d_i} \leq 0.07$.

In conclusion, narrow RTD in multichannel microreactors can only be expected, when the design of gas distributor in front of the microchannel array and the design of the collector behind the channels are optimized.

A difficulty for the experimental characterization is the fact that the fluid distribution in the distributor and collector are comprised in the experimental distribution curve. As the flow in the inlet and outlet regions can be complex, correct

modeling of the complete microdevice with the presented models is hardly possible [14].

An example for measured RTD of gas flow in a stainless steel microstructured device (Figure 3.26) is shown in Figure 3.27. The experiments were carried out with an array of 340 rectangular channels of $300 \times 240 \mu\text{m}$, which were coated with an alumina catalyst. The results prove that the coating was very regular and did not deteriorate the flow behavior. The experimental results can be described satisfactorily with the dispersion model with a Bodenstein number of $Bo = 70$. Compared to predicted RTD for single channels with the Taylor-Aris correlation, the Bo is quite low. This indicates the important influence of the inlet and outlet regions on the overall dispersion. A detailed study of the influence of the gas distributor and collector design on the RTD confirms the discussed findings [14].

3.6.2

RTD of Liquid Flow in Microchannels

Whereas radial diffusion times for gases ($D_m \cong 10^{-5} \text{ m}^2 \text{ s}^{-1}$) in microchannels is in the order of 10^{-2} s , the radial diffusion time for liquids (with $D_m \cong 10^{-9} \text{ m}^2 \text{ s}^{-1}$) is in the order of seconds even in microchannels with diameters of $100 \mu\text{m}$. To reach a narrow RTD ($Bo \geq 100$) in stratified flow, long residence times of $\tau \geq 8 \cdot 10^8 \cdot d_h^2$ (in seconds) are necessary. But, in contrast to the estimations based on the Taylor-Aris correlation (Equation 3.75), experimentally determined RTD are often much

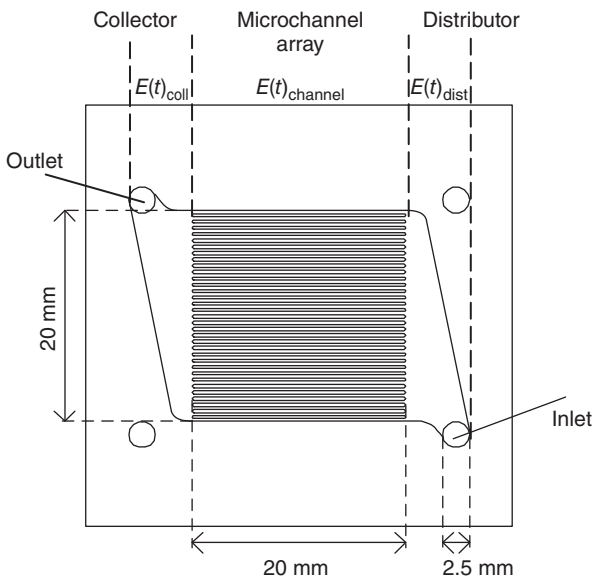


Figure 3.26 Drawing of a microstructured multichannel reactor. Channel: $300 \times 240 \mu\text{m}$. 34 channels/plate; 10 plates. (Institut für Mikrotechnik Mainz, IMM) [15]. (Adapted with permission from Elsevier.)

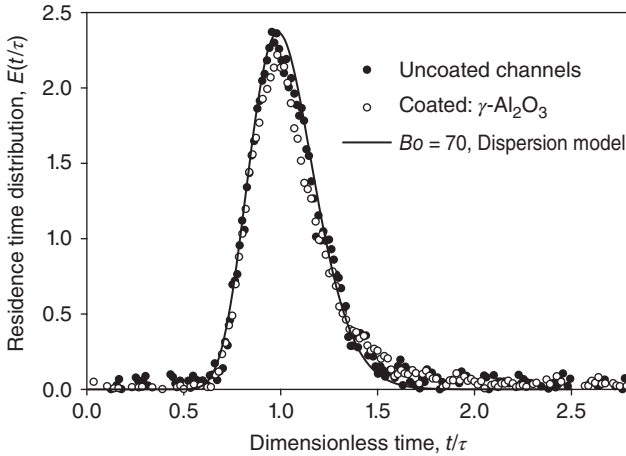
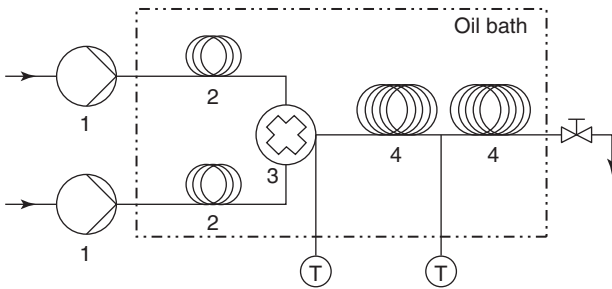


Figure 3.27 Measured residence time distribution in a microstructured device (Figure 3.26): 340 microchannels, space time $\tau = 2.5$ s. [14] (Adapted with permission from Elsevier.)



1. Syringe pump; 2. preheating coil; 3. micromixer; 4. delay pipe

Figure 3.28 Set-up of a microchannel system for ionic liquid synthesis. 1. Syringe pump, 2. preheating coil, 3. micromixer, 4. delay pipe. Adapted from Ref. [16] with permission from Elsevier.)

more narrow. An example is the experimentally determined RTD obtained in a microstructured device for the synthesis of ionic liquids [16]. The experimental set-up used is shown in Figure 3.28. The installation is typical for small-scale continuous chemical synthesis. It consists of high-precision pumps for dosing the reactants, preheater, a micromixer, and a delay channel. An efficient micromixer is essential to ensure fast mixing down to the molecular scale at very short residence times to avoid preliminary reactions eventually accompanied with an uncontrolled temperature increase. The transformation of the reactants occurs in the following delay pipe, where residence times of several minutes can be attained. The micro-tubular reactor consists of a 1.13 m long capillary in the form of a coil with an inner diameter of 1.8 mm. As the studied reaction is of second order and high conversion is warranted, uniform residence time is indispensable for high product yield and reactor performance.

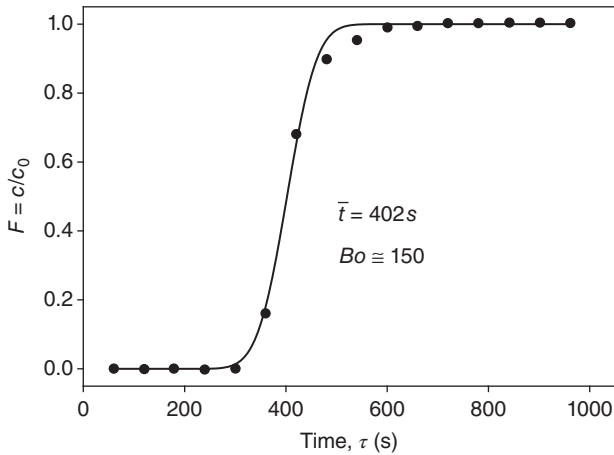


Figure 3.29 F -curve measured by a step-stimuli response and predicted with dispersion model (Equation 3.78. Experimental values taken from Ref. [16].)

The RTD in the tubular reactor was determined experimentally with water as fluid and Brilliant Blue dye as tracer. The tracer was introduced at the reactor inlet in the form of a step function. The concentration of the dye was measured with an UV-vis spectrometer and the response curve is given as F -curve. As the experimental F -curve shown in Figure 3.29 is very steep, a low axial dispersion can be expected. Therefore, RTD will be described with the dispersion model supposing small deviation from plug flow (Equation 3.50). The F -curve valid for small dispersion ($Bo \geq 100$) can be obtained by integrating the RTD given by $E(\theta)$ (Equation 3.50).

$$F = \int_0^\theta E(\theta') d\theta' = \frac{1}{2} \left\{ \operatorname{erf} \left[\sqrt{Bo/4} \cdot \left(\frac{t}{\bar{t}} - 1 \right) \right] - \operatorname{erf}(\sqrt{Bo/4}) \right\} \quad (3.78)$$

The mean residence time, \bar{t} , and the Bo can be obtained by fitting the F -curve (Equation 3.78) to the experimental results.

For the example shown in Figure 3.29 a mean residence time of $402 \text{ s} \pm 0.5\%$ and a Bo of $150 \pm 13\%$ is obtained. This confirms the small dispersion and allows considering the reactor as an ideal plug flow reactor.

On the basis of the Taylor-Aris correlation (Equation 3.75) a Bodenstein number of $Bo \cong 24$ is expected. The experimental results suggest that efficient radial mixing occurs, which may be explained by the used capillary shaped as a coil provoking enhanced radial mixing.

Narrow RTD in an array of plastic capillaries coiled in a spiral form were reported by Hornung and Mackley [17]. The array consisted of up to 19 capillaries in parallel with an inner diameter of $223 \mu\text{m}$ and a length of 10 m. The space time was varied between 30 s and 1.5 h. Experiments using optical fibers for the detection of a tracer dye at the entrance and outlet of the capillaries confirmed near plug flow behavior with Bo up to 220 depending on the flow rate, which could be predicted from the Taylor-Aris correlation for single tubes. Remarkable

is that the inlet flow is evenly distributed over the 19 capillaries thus avoiding maldistribution and broadening of the RTD (Figure 3.30).

As mentioned above, radial mixing is crucial to get narrow RTD. Therefore, the use of passive mixer helps equalizing the radial concentration in the laminar flow domain. It is known that static mixer allows to obtain narrow RTD in tubular reactors even with high viscous media [18]. The beneficial effect of radial mixing can also be expected in microstructured mixers. Bošković *et al.* [19, 20] studied the RTD in three different mixing devices: serpentine channel, split and recombine, and staggered herringbone reactors (SHR) (Table 3.4). They developed and applied an impulse-response technique to characterize the mixers in a wide range of Re between $0.3 < Re < 110$. Serpentine channel reactor (SCR) and split and recombine reactor (SAR) demonstrated a similar behavior. With increasing volumetric flow the variance diminishes. This is shown for the SCR in Figure 3.31 as an example.

Radial mixing in SCR and SAR becomes important mainly at $Re > 30$. The Bo -number at $Re < 30$ is relative low with values in the range of $20 < Bo < 30$ (Figure 3.32). Within this domain, radial mixing seems to be mainly governed by molecular diffusion. For $Re > 30$ Bo increases drastically and reaches values of $Bo \cong 100$ at $Re \cong 100$. In spite of the fact that the space times under these conditions are in the order of 1 s, plug flow behavior is obtained. This fact is quite important for fast chemical transformations leading to high conversions at short residence times.

The SHR shows different RTD characteristics compared to the previous discussed micromixers. Even at very low Re , the main peak of the distribution is quite narrow and symmetric. But, a flat and long tailing is observed [20]. The behavior suggests the presence of a dynamic phase with near plug flow behavior and a

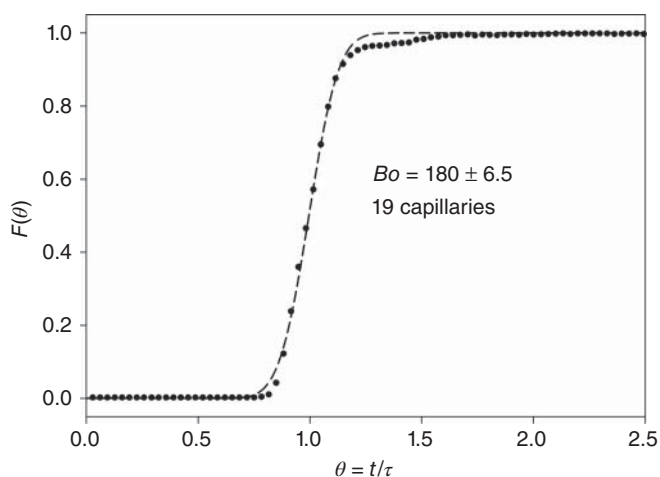





Figure 3.30 Cumulative RTD in a 19-capillary spiral microdevice at 1 ml min^{-1} . Experimental results compared to the dispersion model. (Values taken from Ref. [17].)

Table 3.4 Characteristics and flow conditions for RTD studies [20].

	Split and recombine reactor	Serpentine channel reactor	Staggered herringbone reactor
			
Hydraulic diameter d_h (μm)	400	600	400
Total channel length L_c (mm)	164	233	100
Flow rate \dot{V}_o (ml min^{-1})	$0.025 \leq \dot{V}_o \leq 3$	$0.01 \leq \dot{V}_o \leq 3$	$0.01 \leq \dot{V}_o \leq 3$
Re [-]	$0.3 \leq Re \leq 83$	$0.4 \leq Re \leq 111$	$0.4 \leq Re \leq 111$

Adapted with permission from Wiley.

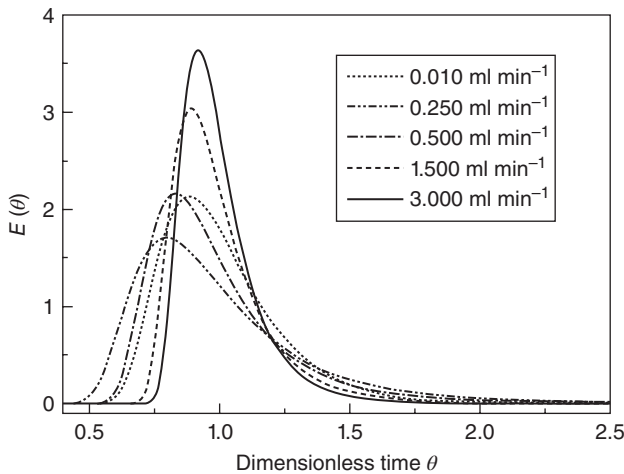


Figure 3.31 Experimentally obtained RTDs of the serpentine channel reactor (SCR). (Adapted from Ref. [20] with permission from Wiley).

very small stagnant phase located in the grooves of the structure. The exchange between these dead zones and the dynamic phase is governed by molecular diffusion, which explains the long tailing.

3.6.3

RTD of Multiphase Flow in Microchannels

Because of the laminar flow in microchannels and the small diffusion coefficient in the order of $10^{-9} \text{ m}^2 \text{ s}^{-1}$, narrow RTD in straight channels at low Re -numbers are not easy to obtain. As the radial diffusion time is long, high axial dispersion is particularly important at short residence times.

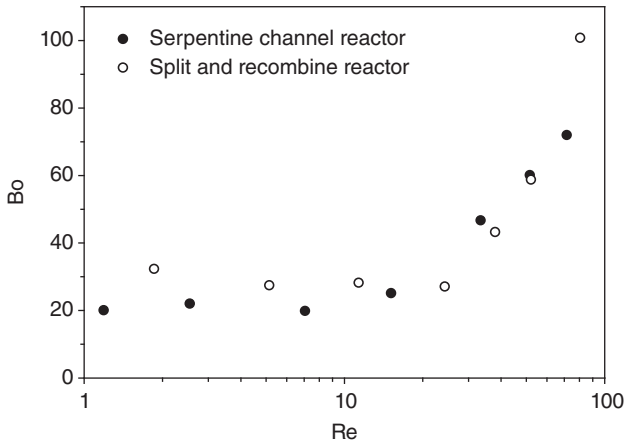


Figure 3.32 Evolution of Bo as function of Re for SAR and SCR micro-mixer. (Data taken from Ref. [20].)

A way to overcome problems related to RTD is the use of multiphase flow (gas–liquid, liquid–liquid). Laminar flow in microchannels permits the easy formation of fluid–fluid slugs (see Chapter 7). Under these conditions, the reaction mixture is present in the form of segments, which are separated by gas bubbles or by a second liquid, immiscible with the reaction phase. In this way, the reacting segments behave as a series of small batch reactors traveling through the channel, thus eliminating the problem of axial dispersion as found in laminar single-phase flow reactors at short residence times. But, the indicated situation is strictly true only if the different segments are completely disconnected from each other. Therefore, the reacting phase must be dispersed in a continuous carrier phase, which is wetting the microchannel walls. This situation is illustrated in Figure 3.33. A cross-junction with three inlets and one outlet is a suitable device for generating regular slug flow. The reactants are introduced in two opposite inlets while the immiscible carrier fluid is introduced through the third inlet generating slug flow.

The experimental proof of this concept is presented by Trachsel *et al.* [22]. They used a microstructured device composed of meandering channels with rectangular cross section, 0.4 mm wide, 0.115 mm high, and 1063 mm long as shown in Figure 3.34.

The authors used a fluorescently labeled tracer, which was injected as impulse. The response of the inlet signal could be followed at different distances downstream from the injection point. Two-phase experiments were carried out by injecting gas as a separating fluid and the results were compared with RTD obtained with single-phase flow. Typical RTD curves for single and multiphase flow are reproduced in Figure 3.35. The experimental results are fitted to the dispersion model supposing open/open boundary conditions (see Figure 3.11, Equation 3.45).

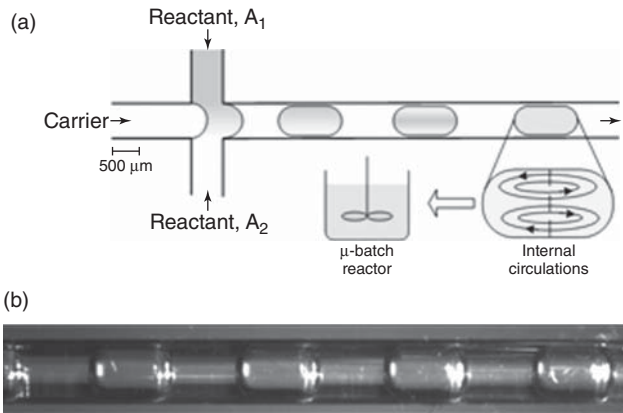


Figure 3.33 Biphasic flow in microchannel for narrow RTD: (a) schematic illustration and (b) monochrome snapshot of slug flow. (Adapted from Ref. [21] with permission from Elsevier.)

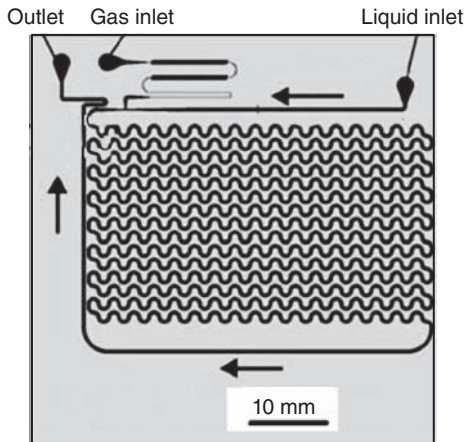


Figure 3.34 Scheme of the microchannel device for RTD studies. (Adapted from Ref. [22] with permission from Elsevier.)

The two-phase flow leads to significant narrower RTD with a Bodenstein number of $Bo = 308 \pm 3$, whereas $Bo = 83 \pm 2$ was estimated from the results obtained for single cell flow (Figure 3.35).

In the presented study, liquid segments are separated by gas bubbles. But the liquid wets the channel wall and forms a small film, which allows communication between the segments and, as a consequence, enables axial dispersion.

The influence of wall film on the RTD in segmented flow was studied in detail by Kuhn *et al.* [23]. The authors used microreactors with a square section of 0.4×0.4 mm and a length of 750 mm. The walls of the silicon-based microdevices were modified by growing a thin silicon oxide layer to get a hydrophilic surface

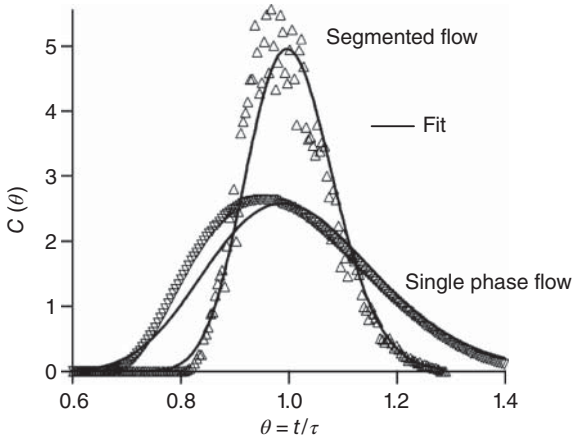


Figure 3.35 Comparison of measured RTD with dispersion model (Equation 3.45). Segmented flow: superficial velocity $u_{\text{liquid}} = 3.6 \text{ mm s}^{-1}$,

$u_{\text{gas}} = 25.2 \text{ mm s}^{-1}$, $\tau = 59 \text{ s}$. Single-phase flow: $u_{\text{liquid}} = 14.9 \text{ mm s}^{-1}$, $\tau = 71 \text{ s}$. (Adapted from Ref. [22] with permission from Elsevier.)

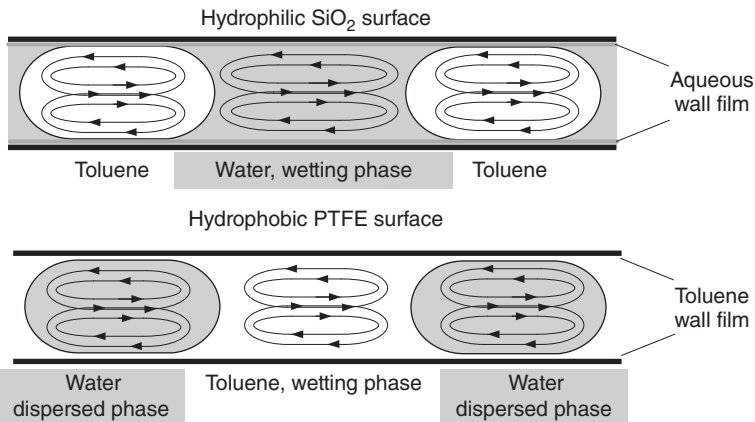


Figure 3.36 Sketch of the phase behavior depending on the wettability of the surface.

or by coating it with a thin PTFE (polytetrafluoroethylene) layer for obtaining a hydrophobic surface. Toluene and water were used as biphasic system. The RTD of the water phase was studied by injecting a pulse of a sodium benzoate solution at the reactor entrance. The response curve was determined by UV-vis spectroscopy. In the silicon-oxide-coated microchannels, water constitutes the continuous phase in which toluene is dispersed. The water segments, separated by toluene slugs, form an aqueous wall film, which allows communicating with each other through axial dispersion. In contrast, in the PTFE-coated microchannel, water is dispersed in the continuous toluene phase. In consequence, the water

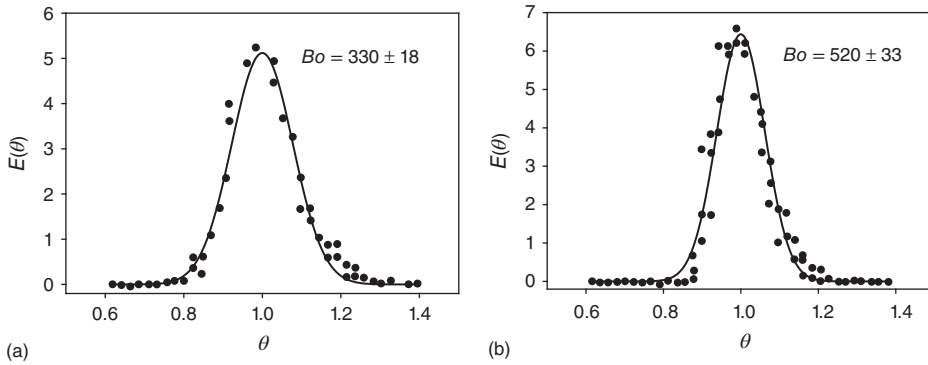


Figure 3.37 Residence time distributions for (a) silicon oxide and (b) PTFE coated microchannels. Flow rate: $12.5 \mu\text{L min}^{-1}$ water, $12.5 \mu\text{L min}^{-1}$ toluene. Solid lines represent the fit of the dispersion model Equation 3.50. (Values taken from Ref. [23]. Adapted with permission Kuhn *et al.* [23]. Copyright (2011) American Chemical Society.)

segments are isolated and can no longer communicate with each other. The described situations are illustrated schematically in Figure 3.36.

In Figure 3.37 the measured RTD for hydrophilic and hydrophobic microchannels are shown. The experimental results can be described with the dispersion model valid for small dispersion (Equation 3.50).

The resulting Bo -numbers estimated by curve fitting was found to be $Bo = 300 \pm 18$ for the hydrophilic channels and $Bo = 520 \pm 33$ for the hydrophobic channels.

The results confirm the beneficial use of segmented flow for realizing plug flow behavior in microstructured reactors. Narrow RTD can be obtained even for short residence times, allowing high performance and product yields for fast chemical reactions.

3.7

List of Symbols

Symbols	Significance	Unit
$c(t)$	Concentration at time t	mol m^{-3}
$E(t)$	Probability function	s^{-1}
E	Dimensionless probability function	—
F	F -curve in RTD	—
$g(t)$	Convolution function	—
N	Number of tanks in cascade	—
n, n_{inj}	Number of moles, amount of non-reacting tracer injected	mol

Symbols	Significance	Unit
$\dot{n}_i, \dot{n}_{i,0}, \dot{n}_{i,L}$	Molar flow rate of species i , at reactor inlet, at length L (outlet)	mol s^{-1}
sk	Skewness	—
\bar{t}, \bar{t}_c	Mean residence time, mean residence time from measured RTD curve for open or semi-open systems	s
$\bar{u}, u_{(r)}, u_{\max}$	Average velocity over cross section, velocity at radial position r , velocity in the center of the tube in laminar flow	m s^{-1}
\bar{X}	Mean conversion for multichannel reactor	—
y	Ratio of radial distance to tube radius	—
Δt	Time interval	s
μ_1, μ_2	Moments of the distribution density function	—
σ^2, σ_c^2	variance of the distribution, variance from measured RTD curve for open or semi-open systems	s^2
$\sigma_\theta^2, \sigma_{\theta c}^2$	variance of the distribution, variance from measured RTD curve for open or semi-open systems	—
θ_c	Dimensionless time from measured RTD curve for open or semi-open systems	—
τ_i	Space time of reactor i	s
χ	Geometrical constant	—

References

- Ham, J.H. and Platzer, B. (2004) Semi-empirical equations for the residence time distributions in disperse systems – part I: continuous phase. *Chem. Eng. Technol.*, **27** (11), 1172–1178.
- Baerns, M., Behr, A., Brehm, A., Gmehling, J., Hofmann, H., Onken, U., and Renken, A. (2006) *Technische Chemie*, 4th edn, Wiley-VCH Verlag GmbH, Weinheim, 733 p.
- Danckwerts, P.V. (1953) Continuous flow systems: distribution of residence times. *Chem. Eng. Sci.*, **2** (1), 1–13.
- Baerns, M., Hinrichsen, K.-O., Hofmann, H., and Renken, A. (2013) in *Chemische Reaktionstechnik. Technische Chemie* (eds M. Baerns, A. Behr, A. Brehm, et al.), Wiley-VCH Verlag GmbH, Weinheim, 736 pp.
- Pallaske, U. (1984) Kritik an zwei bekannten Verweilzeitformeln für das Diffusionsströmungsrohr. *Chem. -Ing. Technol.*, **56**, 46–47.
- Renken, A. and Kashid, M.N. (2012) in *Catalysis: From Molecular to Reactor Design* (eds M. Beller, A. Renken, and R.A.v. Santen), Wiley-VCH Verlag GmbH, Weinheim, pp. 563–628.
- Aris, R. (1955) On the dispersion of a solute in a fluid flowing through a tube. *Proc. R. Soc. London, Ser. A*, **A 235**, 67–77.
- Taylor, G. (1953) Dispersion of soluble matter in solvent flowing slowly through a tube. *Proc. R. Soc. London, Ser. A*, **A 219**, 186–203.
- Aubin, J., Prat, L., Xuereb, C., and Gourdon, C. (2009) Effect of microchannel aspect ratio on residence time distributions and the axial dispersion coefficient. *Chem. Eng. Process.*, **48** (1), 554–559.
- Commence, J.-M., Falk, L., Corriou, J.-P., and Matlosz, M. (2002) Optimal design for flow uniformity in microchannel reactors. *AIChE J.*, **48** (2), 345–358.

11. Delsman, E.R., de Croon, M.H.J.M., Elzinga, G.D., Cobden, P.D., Kramer, G.J., and Schouten, J.C. (2005) The influence of differences between microchannels on microreactor performance. *Chem. Eng. Technol.*, **28** (3), 367–375.
12. Mies, M.J.M., Rebrov, E.V., De Croon, M.H.J., Schouten, J.C., and Ismagilov, I.Z. (2006) Inlet section for providing a uniform flow distribution in a downstream reactor comprises upstream and downstream passage with specifically positioned elongated parallel upstream and downstream channels. WO Patent 2006107206-A2
13. Rebrov, E.V., Schouten, J.C., and de Croon, M.H.J.M. (2011) Single-phase fluid flow distribution and heat transfer in microstructured reactors. *Chem. Eng. Sci.*, **66** (7), 1374–1393.
14. Wibel, W., Wenka, A., Brandner, J.J., and Dittmeyer, R. (2013) Measuring and modeling the residence time distribution of gas flows in multichannel microreactors. *Chem. Eng. J.*, **215-216**, 449–460.
15. Rouge, A., Spoetzl, B., Gebauer, K., Schenk, R., and Renken, A. (2001) Microchannel reactors for fast periodic operation: the catalytic dehydration of isopropanol. *Chem. Eng. Sci.*, **56** (4), 1419–1427.
16. Hu, S., Wang, A., Löwe, H., Li, X., Wang, Y., Li, C., and Yang, D. (2010) Kinetic study of ionic liquid synthesis in a microchannel reactor. *Chem. Eng. J.*, **162** (1), 350–354.
17. Hornung, C.H. and Mackley, M.R. (2009) The measurement and characterisation of residence time distributions for laminar liquid flow in plastic microcapillary arrays. *Chem. Eng. Sci.*, **64** (17), 3889–3902.
18. Flaschel, E., Nguyen, K.T., and Renken, A. (1985) *Proceeding of the 5th European Conference on Mixing, Würzburg*, BHRA, Bedford, p. 549.
19. Bošković, D. and S.L. (2008) Modelling of the residence time distribution in micromixers. *Chem. Eng. J.*, **135** (Suppl. 1), S138–S146.
20. Bošković, D., Loebbecke, S., Gross, G.A., and Koehler, J.M. (2011) Residence time distribution studies in microfluidic mixing structures. *Chem. Eng. Technol.*, **34** (3), 361–370.
21. Kashid, M., Detraz, O., Moya, M.S., Yuranov, I., Prechtel, P., Membrez, J., Renken, A., and Kiwi-Minsker, L. (2013) Micro-batch reactor for catching intermediates and monitoring kinetics of rapid and exothermic homogeneous reactions. *Chem. Eng. J.*, **214**, 149–156.
22. Trachsel, F., Günther, A., Khan, S., and Jensen, K.F. (2005) Measurement of residence time distribution in microfluidic systems. *Chem. Eng. Sci.*, **60** (21), 5729–5737.
23. Kuhn, S., Hartman, R.L., Sultana, M., Nagy, K.D., Marre, S., and Jensen, K.F. (2011) Teflon-coated silicon microreactors: impact on segmented liquid-liquid multiphase flows. *Langmuir*, **27** (10), 6519–6527.